Functional susceptibility of tropical forests to climate change

Jesús Aguirre-Gutiérrez [a,b,*], Erika Berenguer [a,ak], Imma Oliveras [a], David Bauman [a,c], Jose Javier Corral-Rivas [d], Maria Guadalupe Nava-Miranda [d], Sabine Both [e], Josué Edzang Ndong [f], Fidèle Evouna Ondo [f], Natacha N'ssi Bengone [g], Vianet Mihinhou [g], James W. Dalling [h,i], Katherine Heineman [i], Axa Figueiredo [j], Roy González-M [k], Natalia Norden [k], Ana Belén Hurtado-M [k], Diego González [k], Beatriz Salgado-Negret [l], Simone Matias Reis [a,m], Marina Maria Moraes de Seixas [n], William Farfan-Rios [o,p,q], Alexander Shenkin [a,] Terhi Riutta [a,r], Cécile A. J. Girardin [a], Sam Moore [a,] Kate Abernethy [s,t], Gregory P. Asner [u], Lisa Patrick Bentley [v], David F.R.P. Burslem [w], Lucas A. Cernusak [x], Brian J. Enquist [y], Robert M. Ewers [z], Joice Ferreira [aa], Kathryn J. Jeffery [z], Carlos A. Joly [ab], Ben Hur Marimon-Junior [m], Roberta E. Martin [u], Paulo S. Morandi [m], Oliver L. Phillips [ac], Amy C. Bennett [ac], Simon L. Lewis [ac,ad], Carlos A. Quesada [ae], Beatriz Schwantes Marimon [m], W. Daniel Kissling [af,] Miles Silman [ag], Yit Arn The [ah], Lee J. T. White [g,s,t], Norma Salinas [a,ai], David A. Coomes [aj], Jos Barlow [ak], Stephen Adu-Bredu [al], Yadvinder Malhi [a]

[a]Environmental Change Institute, School of Geography and the Environment, University of Oxford, Oxford, UK
[b]Biodiversity Dynamics, Naturalis Biodiversity Center, Leiden, The Netherlands
[c]Smithsonian Environmental Research Center, Edgewater, Maryland 21037, USA.
[d]Facultad de Ciencias Forestales, Universidad Juárez del Estado de Durango, México
[e]Environmental and Rural Science, University of New England, Armidale, 2351 NSW, Australia
[f]Agence Nationale des Parcs Nationaux, BP20379, Libreville, Gabon
[g]Ministère des Eaux, des Forêts, de la Mer et de L'Environnement, Libreville, Gabon
[h]Smithsonian Tropical Research Institute, Panama City, Republic of Panama
[i]Department of Plant Biology, University of Illinois, Urbana, IL, USA
[j]National Institute of Amazonian Research – INPA. C.P. 2223, 69080-971, Manaus, AM, Brazil
[k]Programa Ciencias Básicas de la Biodiversidad, Instituto de Investigación de Recursos Biológicos Alexander von Humboldt, Cr. 1 # 16-20, Bogotá, Colombia
[l]Departamento de Biología, Universidad Nacional de Colombia, Bogotá, Colombia
[m]Laboratório de Ecologia Vegetal (LABEV), Universidade do Estado de Mato Grosso, Nova Xavantina, Brazil
[n]Embrapa Amazônia Oriental, Trav. Dr. Enéas Pinheiro, s/n, CP 48, 66095-100 Belém, PA, Brazil
[o]Living Earth Collaborative, Washington University in Saint Louis, St. Louis, MO, USA
[p]Center for Conservation and Sustainable Development, Missouri Botanical Garden, St. Louis, MO, USA
[q]Herbario Vargas (CUZ), Escuela Profesional de Biología, Universidad Nacional de San Antonio Abad del Cusco, Cusco, Peru
[r]College of Life Sciences, University of Exeter, Exeter, UK
[s]Institut de Recherche en Écologie Tropicale, Libreville, Gabon.
[t]Biological and Environmental Sciences, University of Stirling, Stirling, UK.
[u]Center for Global Discovery and Conservation Science, Arizona State University, Tempe, AZ, United States
[v]Department of Biology, Sonoma State University, 1801 East Cotati Avenue, Rohnert Park, CA 94928, USA
[w]School of Biological Sciences, University of Aberdeen, Aberdeen, UK
[x]College of Science and Engineering, James Cook University, Cairns, Qld, 4878 Australia
[y]Department of Ecology and Evolutionary Biology, University of Arizona, Tucson, Arizona, USA
[z]Department of Life Sciences, Imperial College London, Ascot, UK
[aa]MCT/Museu Paraense Emílio Goeldi, Av. Magalhães Barata376, São Braz, 66040-170, Belém, PA, Brazil
[ab]Universidade Estadual de Campinas, Instituto de Biologia, Departamento de Biologia Vegetal, Campinas, São Paulo, Brazil
[ac]Ecology and Global Change, School of Geography, University of Leeds, Leeds, UK
[ad]Department of Geography, University College London, London, UK
[ae]Coordenação de Dinâmica Ambiental, Instituto Nacional de Pesquisas da Amazônia, Manaus, Brazil
[af]Institute for Biodiversity and Ecosystem Dynamics (IBED), University of Amsterdam, Amsterdam, The Netherlands
[ag]Department of Biology, Wake Forest University, Winston-Salem, NC 27109, USA
[ah]School of Natural and Environmental Sciences, Newcastle University, Newcastle Upon Tyne, UK
[ai]Sección Química, Pontificia Universidad Católica del Perú, Avenida Universitaria 1801, San Miguel, Lima 32, Peru
[aj]Department of Plant Sciences and Conservation Research Institute, University of Cambridge, Cambridge CB2 3QZ, UK
[ak]Lancaster Environment Centre, Lancaster University, Lancaster LA1 4YQ, UK
[al]CSIR-Forestry Research Institute of Ghana, University P.O. Box 63, Kumasi, Ghana
*Corresponding author

ABSTRACT

Tropical forests are some of the most biodiverse ecosystems in the world, yet their functioning is threatened by anthropogenic disturbances and climate change. Global actions to conserve tropical forests could be enhanced by targeting areas with low levels of functional diversity and functional redundancy, and therefore with diminished capacity to respond to a changing environment. Here, we create estimates of plant functional diversity and redundancy across the tropics by combining a dataset of 16 morphological, chemical and photosynthetic plant traits sampled from 2461 individual trees from 74 sites distributed across four continents, together with local climate data for the last half century. Our findings suggest a strong link between climate and functional diversity and redundancy with the three trait groups responding similarly across the tropics and climate gradient. We show that drier tropical forests are overall less functionally diverse than wetter forests and that functional redundancy declines with increasing soil water and vapour pressure deficits. Areas with high functional diversity and high functional redundancy tend to better maintain ecosystem functioning, such as aboveground biomass, after extreme weather events. Our predictions suggest that the lower functional diversity and lower functional redundancy of drier tropical forests, in comparison to wetter forests, may leave them more at risk of shifting towards alternative states in face of further declines in water availability across tropical regions.

INTRODUCTION

Tropical forests are amongst the most biodiverse ecosystems on the planet [1], they harbour more than 50% of global biodiversity including between 67-88% of all tree species [2] and are responsible for more than 30% of terrestrial productivity [3]. Given the large distribution of tropical forests on earth, small but widespread changes in their tree community composition can have global impacts in the removal of CO_2 from the atmosphere [4]. Tropical forests are also essential to help mitigate the effects of climate change, as intact tropical forests are carbon sinks of around 1.26 Pg C yr^{-1} [5]. However, carbon storage can be negatively impacted by changes in water availability [6]. For example, the Amazon forest, which contains close to 123 Pg C of above and belowground biomass[7] lost 1.2-1.6 Pg C [8] – the equivalent of 1% of its total carbon stocks [9] – during the extreme drought of 2005 and it is now suggested to be a carbon source [10]. Besides impacting the carbon storage capacity of forests, changes in climate mean states and variability are key potential drivers of biodiversity declines around the world [11, 12]. Understanding how climate may affect tropical forests’ capacity to store carbon thereby requires evaluation of how plants respond to drought stress. To do so, the Maximum Climatic Water Deficit (MCWD) and Vapour Pressure Deficit (VPD) are two fundamental proxies of hydric stress for plants [13, 14], with increases in VPD leading to greater plant transpiration stress [15, 16]. Although it has been generally expected that communities historically adapted to high MCWD and VPD should be better adapted to increasing drier conditions, it could also be that such communities might already be at their climatic physiological limits and thus further droughts may increase water stress to such an extent that they are driven towards alternative states [17, 18]. To disentangle these two possibilities, evaluating functional trait composition may provide clues on their possible historical adaptations to water stress conditions [19, 20]. Although changes in MCWD and VPD are prominent features of climate change across tropical forests, detailed analyses that show their relationship with plant morphology/structure, leaf chemistry and photosynthesis related traits across climatic and elevation gradients at a pantropical scale remain scarce. Thus, understanding the functional-climatic gradients relationship is key to disentangling the long-term role of tropical forests for mitigating climate change and is crucial for deciphering the resilience of key ecosystem properties such as diversity and carbon stocks under a changing climate.

Ecosystem resilience may increase through different pathways, for example, by species having the same traits that affect a given ecosystem process, such as carbon capture, but different traits to respond to environmental changes, such as droughts. Arguably functional traits may respond differently to diverse drivers of change (e.g. temperature or precipitation change) which may be reflected in trait diversity but not necessarily in species richness [21] given that there is not always a tight relation between species richness and functional trait diversity [22, 23]. According to the biodiversity-ecosystem functioning insurance hypothesis [24], ecosystem functions should be less affected by a changing environment when 1) the ecosystem possesses both high functional diversity (e.g. large range of trait values; FD), 2) but also a wide set of species with similar functional characteristics [24] conferring the system with high functional redundancy (FRed) [25, 26]. Thus, in communities with high functional diversity and high functional redundancy, the loss of a given species is less likely to result in the disruption of the ecosystem function [27], as other species will probably continue carrying out the same functions, substituting the lost species [28, 29]. High FD and high FRed may enhance the temporal stability of ecosystem functions (e.g., biomass productivity) [30] and thus provide a buffering effect against environmental changes [24], conferring higher resilience. Nonetheless, these hypotheses have never been tested across the tropics, and the role of FD and FRed for maintaining the tropical forests ability to capture and store carbon remains to be tested and quantified at this global scale. Quantifying the FD and FRed is crucial to advancing our understanding of the resilience of these forests in the Anthropocene.

Here, we address this knowledge gap by combining a new pantropical dataset of 16 plant traits related to morphology/structure (leaf area, leaf dry and fresh mass, leaf dry matter content, leaf water content, specific leaf area, leaf thickness, wood density), foliar nutrients (leaf calcium, potassium, magnesium, nitrogen and phosphorus content) and photosynthesis (photosynthetic rate, dark respiration). These plant traits are hypothesised to be of importance for tropical forests to adapt or respond to a drying climate (see Table S1 for a description of their hypothesised importance). The importance of such traits relies on their influence on the capacity of species to capture energy for growth and conserve resources (e.g. water) for survival under stressful environmental conditions, such as droughts, and have been shown to change in response to a changing climate [31, 32, 33]. The plant traits were collected from 2461 individual trees belonging to 1611 species distributed across 74 plots that contained 32,464 individual trees equal to or greater than 10 cm diameter at breast height from 2497 species (Fig. S1, Table S2, See Methods). The vegetation plots are free of obvious local anthropogenic disturbance (i.e., far from forest edges, and no evidence of logging or fires) and cover a wide range of the climatic conditions found across tropical and subtropical dry and moist broadleaf forests (Fig. S2; Fig. S3). This dataset was combined with estimates of MCWD and VPD from 1958-2017 and of soil chemistry (cation exchange capacity) and texture (clay content) (Fig. S3).

We address three fundamental questions: 1) Does the long-term mean ambient water stress environment (MCWD and VPD) or its changes (ΔMCWD and ΔVPD) over the last half-century determine current functional diversity (Fig. S3)? First, we examine the relationship between the functional diversity (here calculated as functional dispersion[34]) and redundancy levels across tropical regions. 2) What is the spatial distribution of functional diversity and redundancy across tropical forests? 3) Is there a relationship between functional diversity or functional redundancy and one metric of ecosystem functioning (above ground biomass) during extreme drought events? We expect that: 1) Communities that are found in drier climate conditions and that have experienced stronger decreases in water availability across the last half century will be less functionally diverse but may be more functionally redundant as a result of climate filtering for better adapted traits than communities in less extreme conditions such as wetter forests; 2) Across the full spatial distribution of tropical forests, tropical wet forests communities, which are more species-rich than drier tropical forests, have higher functional diversity given a broader set of ecological strategies available as a result of more stable and favourable climate and soil conditions; 3) There is a positive relationship between functional diversity, functional redundancy and ecosystem functioning (i.e. above ground biomass) as more functionally diverse and redundant communities may attenuate the negative effects of a changing climate and may be therefore be considered to be more resilient.

Results

Functional diversity and redundancy across tropical forests as a proxy for their susceptibility to climate change

Fundamental knowledge on the climate-FD and climate-FRed relationships across tropical forest ecosystems has been missing. To fill this knowledge gap, we calculated, for vegetation plots distributed across the tropics, the FD and FRed for morphological/structural, leaf chemistry and photosynthetic traits that are hypothesised to be of importance for tropical forests to respond to a drying climate. The selected traits play a role in plant establishment, growth and/or survival [19, 20, 35] (Table S1). Then, we investigated variation in FD and FRed across tropical forests by modelling their relation with MCWD, VPD and their interaction, the ΔMCWD and ΔVPD and their interaction (see Methods section), where more positive values in MCWD and VPD reflect stronger water deficits. In our models, we also accounted for soil characteristics (see Methods) such as texture (Clay %) and chemistry (cation exchange capacity, CEC). Soils high in clay content may have high water holding capacity over longer periods of time which is important for vegetation under drought conditions [31]. Moreover, it is widely acknowledged that tropical forests in drier regions are generally associated with soils that are richer in nutrients in comparison to wet tropical forests [36]. The feedbacks between soil–rainfall and their effects on plant distributions could be disrupted under a changing climate and therefore have adverse effects on the functioning of tropical forest ecosystems. A principal component analysis (PCA) of climate conditions (long-term trends and recent changes) indicated that the first two axes explained 71.3% of the variation among plots (Fig. S4a) and the first two axes of the soil-based PCA (with soil chemistry and texture) account for 83% of the variation among plots (Fig. S4b).

Based on the long-term mean MCWD, our results show that drier tropical forests are clearly morphologically less diverse (*slope*= -0.18 [-0.31, -0.05], median and 90% highest density intervals) than wet forests (Table S2). The effect of MCWD on morphological FD was modulated by atmospheric VPD, where the FD of communities with low VPD (blue fitted line in Fig. 1a) strongly decreased as MCWD increased, but FD tended to increase with MCWD in communities where VPD was high (red fitted line in Fig. 1a). Morphological/structural FD increased linearly with increases in clay content (*slope*= 0.08 [0.01, 0.16]; Fig. 1b). Foliar nutrients FD also tended to decrease towards drier forests (*slope*= -0.15 [-0.24, -0.05]; Fig. 1c). Overall, foliar nutrients FD increased towards communities with higher soil CEC (*slope*= 0.17 [0.12, 0.22]; Fig. 1d), while photosynthetic FD also increased towards areas that experienced stronger increases in MCWD (*slope*= 0.14 [0.02, 0.25]; Fig. 1e) but did not respond to the long-term mean MCWD. For the trait groups (morphology, nutrients, photosynthesis) for which a clear relationship with climate and soil was found (90% Highest Density Interval, HDI, of the posterior distribution does not overlap 0; Table S3), the models explained (R^2) 44%, 75% and 75% of the variation in morphology/structure, nutrients and photosynthetic FD, respectively. The models of FRed as a function of climate and soil explained 53%, 73% and 33% of the variation in morphology/structure, nutrients and photosynthetic functional redundancy respectively across the tropical forest.

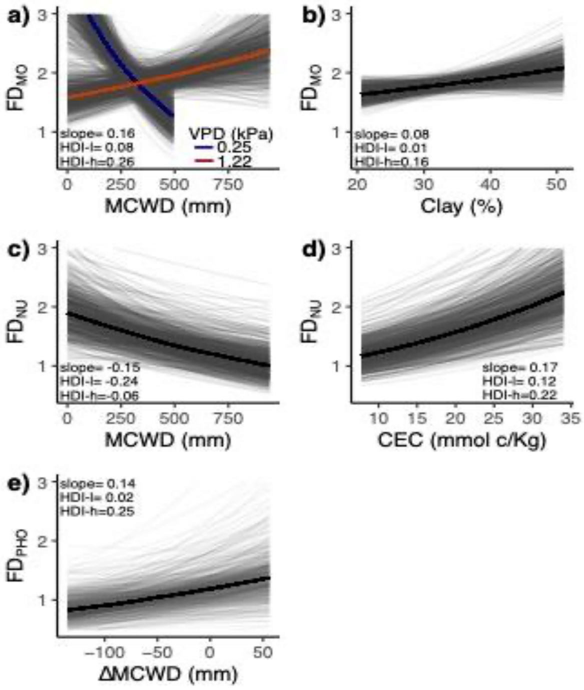

Figure 1. Long-term water availability and its recent changes and soil conditions drive functional diversity of morphological (a, b), leaf nutrients (c-d) and photosynthetic (e) plant traits across the tropics. Only climatic variables with a clearly important relationship (90% Highest Density Interval, HDI, of the posterior distribution does not overlap 0) with functional diversity (FD) are shown. Models for each group (morphology/structure, leaf nutrients, photosynthetic) were fitted as a function of long-term and recent changes in climate and of soil chemistry

(CEC) and texture (Clay). Thick black lines show the average response and shaded lines show 300 random draws from the model posterior distribution representing variability of the expected model fit. The blue fitted line in a) shows the effect of MCWD at the lowest value of VPD and the red fitted line at the highest values of VPD. Larger positive values in MCWD and VPD reflect stronger water deficits. MCWD: maximum climatic water deficit, VPD: vapour pressure deficit, CEC: cation exchange capacity. Δ: change. For details about the single traits that form each of the groups (MO: morphology/structure, NU: leaf nutrients, PHO: photosynthetic) see Table S1. For full statistical results see Table S3.

The FRed models (Table S3) showed that redundancy of morphological/structural (*slope*= -0.06 [-0.11, -0.01]) traits declines with higher long-term mean MCWD and that photosynthetic FRed declines as long-term VPD increases (*slope*= -0.11 [-0.23, -0.01]; Fig. 2a and Fig. 2e respectively). While redundancy of morphological/structural and foliar nutrients traits decreased with increases in MCWD through time (ΔMCWD) in areas that also increased the most in VPD (ΔVPD; Fig. 2b and Fig. 2d red fitted line) the opposite was predicted for areas that experienced larger increases in MCWD but smallest increases in VPD (Fig. 2b and Fig. 2d blue fitted line). FRed of morphological/structural traits also tended to decrease with increases in soil clay content (*slope*= -0.04 [-0.07, -0.003]; Fig. 2c).

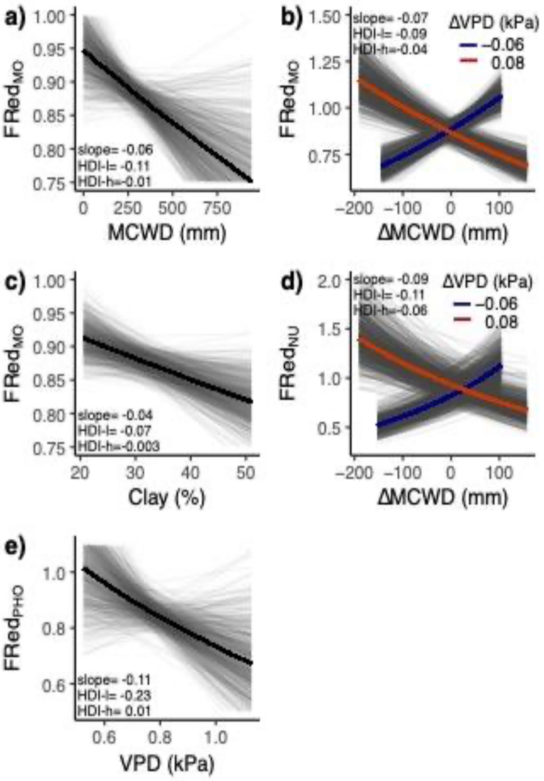

Figure 2. Long-term water availability and its recent changes and soil texture drive functional redundancy of morphological (a-c), leaf nutrients (d) and photosynthetic (e) plant traits across the tropics. Only climatic variables with a clearly important relationship (90% Highest Density Interval, HDI, of the posterior distribution does not overlap 0) with functional redundancy are shown but in e) where the effect of VPD on FRedPHO is marginal. Models for each group (morphology/structure, leaf nutrients, photosynthetic) were fitted as a function of long-term and changes in climate and of soil chemistry (CEC) and texture (Clay). Thick black lines show the average response and shaded lines show 300 random draws from the model posterior distribution representing variability of the expected model fit. The blue fitted line in b) and d) shows the effect of ΔMCWD at the largest decrease in ΔVPD and the red fitted line at the larger increase in ΔVPD. Larger positive values in MCWD reflect stronger water deficits. MCWD: maximum climatic water deficit, VPD: vapour pressure deficit, Δ: change. For details about the single traits that form each of the groups (MO: morphology/structure, NU: leaf nutrients, PHO: photosynthetic) see Table S1. For full statistical results see Table S3.

Mapping functional diversity and functional redundancy across tropical forests

Based on our understanding of the relation of FD and FRed of morphological/structural, leaf nutrients and photosynthetic trait groups with climate and soil (Fig. 1 and Fig. 2), and to fill the knowledge gap on the pantropical distribution of functional diversity and redundancy we created pantropical maps of both FD (Fig. 3) and FRed (Fig. 4) distribution. With our map predictions we aim to uncover the locations of forests with potentially higher and lower resilience to a changing climate. To this end, we used the statistical models built above (Table S3) to predict FD and FRed across the pantropical dry and moist broadleaf forests, for which our field sampling locations have a wide representation of the climatic conditions across those tropical forests (Fig. S2; Fig. S5 and Fig. S6). Based on the FD and FRed predictions, we calculated the percent area that had 'low', 'intermediate' and 'high' diversity and redundancy for each trait group (see methods). We also created bivariate maps that combine the FD and FRed scores in a single map to visualise where FD and FRed are both maximized and minimized across the tropics (Fig. 5). We further developed the same statistical models as described above but by removing from the analysis all plots from each continent (Asia and Australia out at the same time) to determine which regions have higher contribution to determining the observed spatial predictions (those of Fig. 5). For morphology/structure, foliar nutrients and photosynthesis we found high correlations between the bivariate maps developed with the full dataset and when Asia and Australia were left out (*r*= 0.96, 0.82 and 0.94; Fig. S7, Fig. S8, and Fig. S9 respectively; Also Fig. S10). For morphology/structure and photosynthesis there were also high correlations between the patterns based on the full dataset and those based on the one where Africa was removed (*r*= 0.92 and 0.93 respectively; Fig. S7 and Fig. S9 respectively). Low correlations between the maps generated with the full dataset and those based on smaller datasets depict those regions contributed significantly for the full model predictions (Fig. S10), which is also correlated to the number of observations available for each continent (Table S2 and Table S4).

As predicted, our results show that wetter tropical forests tend to be more functionally diverse than drier tropical forests, especially for morphological/ structural traits and foliar nutrients traits, but also more functionally redundant for foliar nutrients and photosynthetic traits than drier tropical forests (Fig. 3 and Fig. 4). While FD levels across our sampling locations are not significantly related to their taxonomic diversity (number of species, genera and families; *P-val* > 0.05), FRed$_{NU}$ appears to be positively correlated to taxonomic diversity (*P-val* < 0.05; Table S5). Our results suggest that given the lower FD (Fig. 3) and FRed (Fig. 4) of drier tropical forests for most of the analysed trait groups, these forests may be more at risk in the face of further water availability reductions.

The bivariate predictions maps combining FD and FRed (Fig. 5) highlight how wet tropical regions, such as the Western Amazon, Central Africa, and several regions in South East Asia maintain high functional diversity and high functional redundancy of morphological/structural (FD$_{MO}$ max=3.5, FRed$_{MO}$ max=1.5) and leaf nutrients traits (FD$_{NU}$ max=2.5, FRed$_{NU}$ max=1.5), and also in several wet regions for leaf photosynthetic traits (FD$_{PHO}$ max=2.5, FRed$_{PHO}$ max=1.5). We expect these wet tropical regions to be more resilient to a changing climate given their large combined FD (Fig. 3) and FRed (Fig. 4). To evaluate which are the different levels FD and FRed across tropical and subtropical dry and moist broadleaf forests, we distinguished low, intermediate and high scores based on the range of the spatial predictions (Table S6; see methods section). We predicted that only 2.4% of the tropical and subtropical dry and moist broadleaf forests have high morphological FD and 2.3% high morphological FRed. In contrast, the drier tropical forests show a functional diversity of morphological/structural traits that reach only about half of that in the wet tropics (FD$_{MO}$ min=~1.5) and some of the lowest FRed (<0.6). From the total area of tropical and subtropical dry and moist broadleaf forests, 30.4% shows low morphological/structural FD and 5.5% have low morphological/structural FRed. Moreover, FD and FRed of leaf nutrients traits are lowest to intermediate across the tropical dry forest regions, such as the southernmost parts of the forests in Brazil, in parts of Mexico, and West Africa (Fig. 3 and Fig. 4).

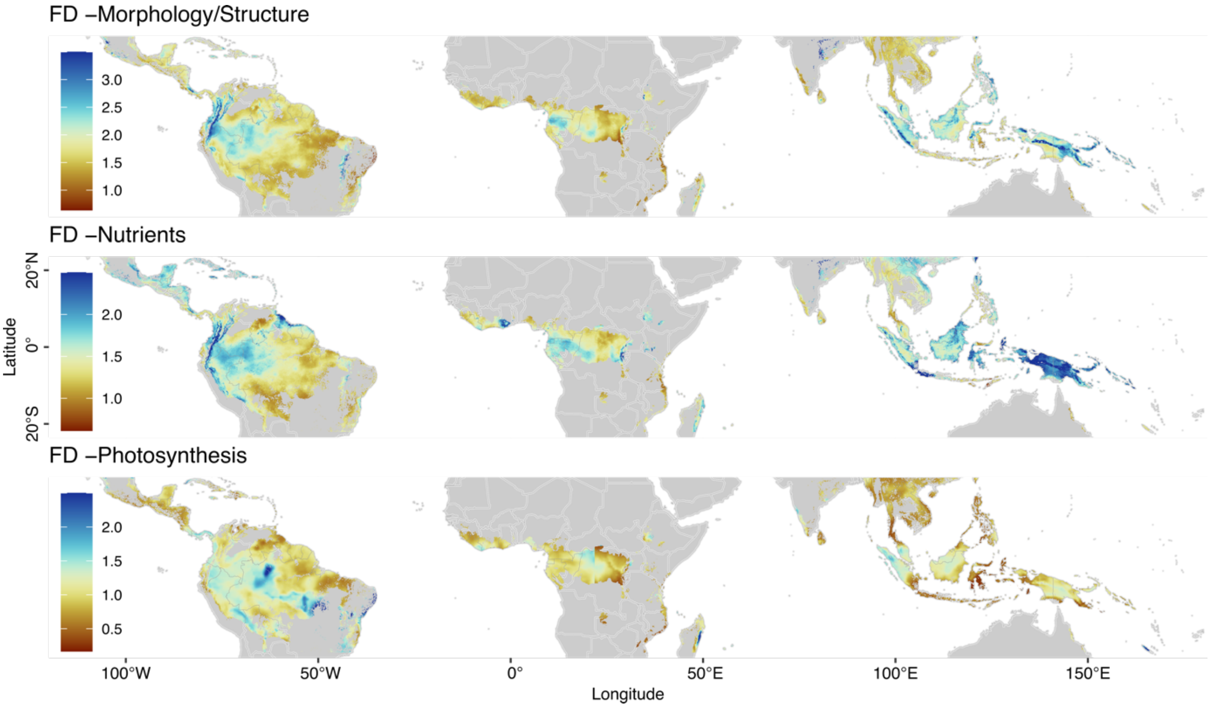

Figure 3. Global predictions of functional diversity (FD) for morphological/structural (top panel), leaf nutrients (middle panel) and photosynthetic (bottom panel) traits across the tropical and subtropical dry and moist broadleaf forests. Dark brown colours depict areas where FD is lowest, light brown and light blue where FD is intermediate and dark blue where FD is predicted to be highest. Functional diversity predictions across the tropics were made using the statistical models for which details are shown in Table S3. The location of field sites whose data informed this analysis is shown in Figure S5.

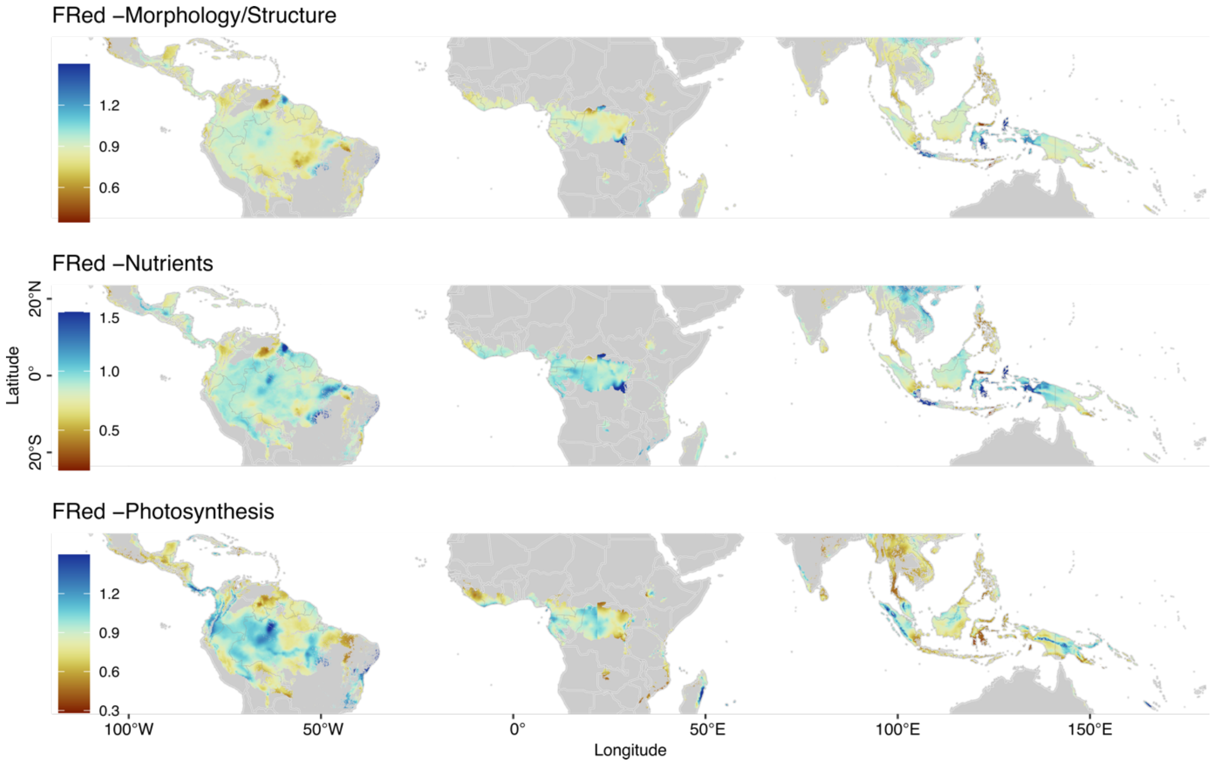

Figure 4. Global predictions of functional redundancy (FRed) for morphological/structural (top panel), leaf nutrients (middle panel) and photosynthetic (bottom panel) traits across the tropical and subtropical dry and moist broadleaf forests. Dark brown colours depict areas where FRed is lowest, light brown and light blue where FRed is intermediate and dark blue where FRed is predicted to be highest. Functional redundancy predictions across the tropics were made using the statistical models for which details are shown in Table S3.

While 14.8% of the forest area has low foliar nutrients FD and 3.7% low FRed, 14.1% shows high nutrients FD and 7% high FRed. Drier tropical forests in Western Mexico, the southern forest portion of Brazil and parts of central and West Africa show intermediate to high photosynthetic FD (max=2.5) but they also tend to show intermediate to low levels of FRed (FRed$_{Pho}$ min=0.3). However, photosynthesis FD and FRed do not seem to have a clear difference between wetter and drier forests. About 36.8% of the tropical and subtropical dry and moist broadleaf forest area is predicted to have low photosynthetic FD and 16.9% to have low photosynthetic FRed, while only 2.4% is expected to have high photosynthetic FD and 6.8% high photosynthetic FRed. Overall, a large amount of forest area has intermediate photosynthetic FD and/or FRed levels (60.7% and 76.3% respectively). The bivariate FD-FRed predictions show that most tropical forests across West Amazon and Central Africa maximise their morphological and photosynthesis FD and FRed, while a smaller area of western South America maximises nutrients FD and FRed (Fig. 5). In general forests in drier areas show lower FD and FRed combined scores (grey colour; Fig. 5 bottom panel) for the three functional groups (morphology/structure, nutrients and photosynthesis) but this is more evident for the photosynthesis traits (Fig. 5).

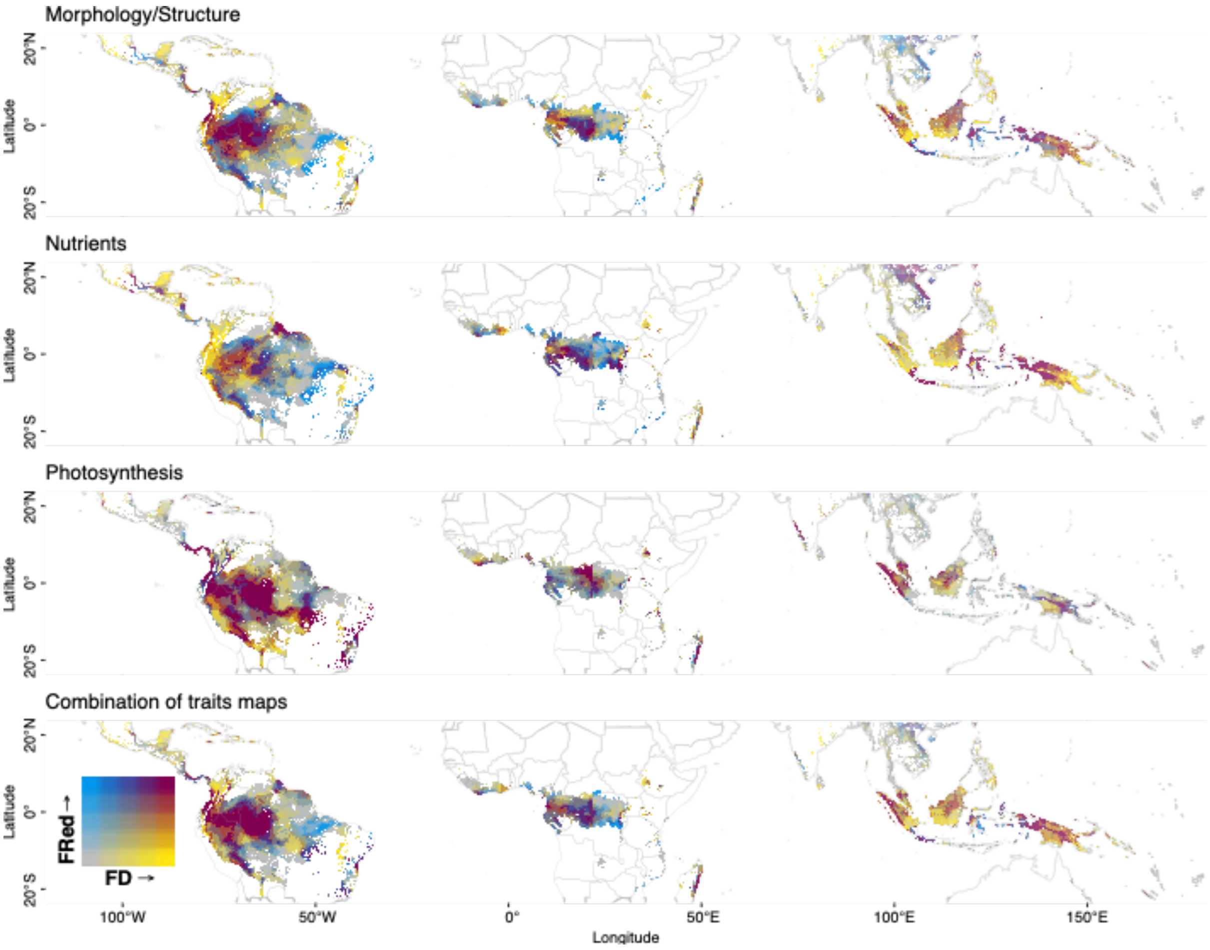

Figure 5. Global bivariate maps combining the scores of the Functional Diversity (FD) and Functional Redundancy (FRed) for morphological/structural (top panel), leaf nutrients (second panel) and photosynthetic (third panel) traits across the tropical and subtropical dry and moist broadleaf forests. The bottom panel shows the combination of the morphological/structural, nutrient and photosynthesis bivariate maps, after standardizing (with values 0 to 1) and summing them to obtain a general bivariate map of global functional diversity and functional redundancy. Purple-red colours depict areas where both FD and FRed are highest, while yellow points to areas with higher FD and blue to areas with higher FRed. Gray colours show areas where both FD and FRed are predicted to be lowest. See full details of the statistical models underlying these predictions in Table S3.

Testing the link between functional diversity, functional redundancy and resilience in ecosystem functions under climate change

We tested to what extent the long-term FD and FRed model predictions (Fig. 3 and Fig. 4), could capture the functioning of tropical forests after climatic disturbances such as El Niño events. By obtaining the above ground biomass data (AGB) from a set of 86 vegetation plots in tropical Africa before and after the 2015 El Niño event [37], we calculated the change in aboveground biomass (ΔAGB) and modelled it as a function of the predicted long-term FD and FRed map scores. Bennett et al. [37] did not detect a strong decline in AGB for most forests they analysed after the 2015 El Niño event. We show that, on average, smaller decreases or larger increases in AGB (Fig. 6; Table S7) can be found at locations that are predicted to have higher long-term FD and FRed of morphology/structure (*slope*= 1.97, [0.28, 3.65]; Fig. 6a) and nutrients traits (*slope*= 2.94, [0.25, 5.69]; Fig. 6b) and also higher FRed of photosynthesis traits (*slope*= 2.96, [0.94, 5.13]; Fig. 6d) (Table S9). The effect of FD_{NU} on ΔAGB was mediated by recent changes in MCWD (ΔMCWD), with positive FD_{NU} effects found in areas that experienced larger increases in mean MCWD (Fig. 6b). There was no strong effect of FD_{PHO} in areas where ΔVPD was smaller (blue fitted line in Fig. 6c) but the effect became negative for areas where ΔVPD was larger (becoming drier, red fitted line in Fig. 6c). The effect of $FRed_{NU}$ on ΔAGB was mediated by ΔMCWD with a positive effect only in regions that experienced increases in water availability (Fig. 6e blue fitted line; *slope*= 2.94 [0.25, 5.69]).

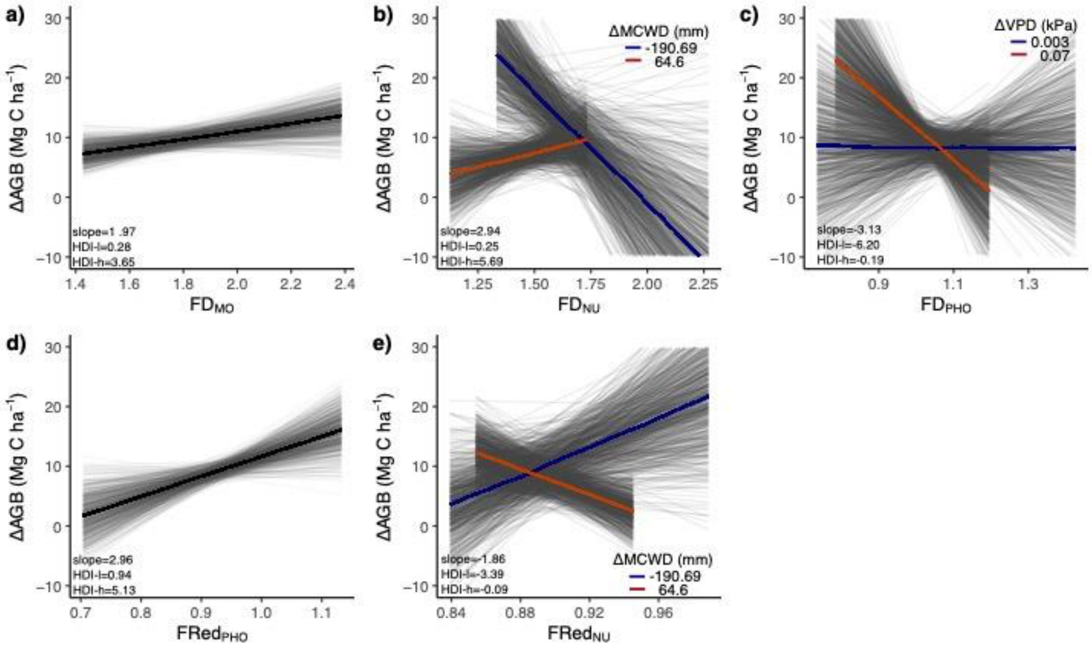

Figure 6. The strength of changes in aboveground biomass (ΔAGB) after extreme events such as the 2015 El Niño (from Bennett et al. [37]) are related to the local functional diversity (FD; a-c) and functional redundancy (FRed; d-e) for sites in Africa. The x axis shows the FD or FRed scores for the morphological/structural (MO), nutrients (NU) and photosynthetic (PHO) traits as extracted from Fig. 3 and Fig. 4 and the Y axis shows the relation with ΔAGB. The ΔAGB shows a clear relation (90% Highest Density Interval, HDI, does not overlap 0) with the diversity indices (Table S7). Thick black lines show the average response and grey shaded lines show 700 random draws from the posterior distribution representing variability of the expected model fit. The blue fitted line in b) shows the effect of FD_{NU} at the largest decrease in ΔMCWD and the red fitted line at the larger increase in ΔMCWD. The blue fitted line in c) shows the effect of FD_{PHO} at the largest decrease in ΔVPD and the red fitted line at the larger increase in ΔVPD. In e) the effect of $FRed_{NU}$ is shown for the largest decrease in ΔMCWD with the blue fitted line and the red fitted line shows the effect at the larger increase in ΔMCWD. The FD and FRed scores for each trait group (i.e. morphology/structure, nutrients and photosynthetic) are predictions extracted from Fig. 3 and Fig. 4 for the vegetation plots where the ΔAGB was collected. Only model covariates with a clear relationship with the ΔAGB are shown. For full statistical results see Table S7.

Discussion

Changes in forest cover affect the local surface temperature by means of the exchanges of water and energy[38]. At the same time climate change is altering land conditions affecting the regional climate and in the near future global warming is likely to cause the emergence of unprecedented climatic conditions in tropical regions [38]. Therefore, determining the distribution of more and less resilient tropical forests (e.g. regarding the maintenance of their functioning) to a changing climate and understanding the mechanisms causing such changes in resilience is pivotal for the conservation of biodiversity and ecosystem functioning.

Theory on niche complementarity predicts that more diverse systems make more efficient use of ecosystem properties given the complementarity of species in the use of resources available [39, 40]. Such complementarity may also increase the performance of diverse communities in the face of more stressful environments given facilitative interaction between species [41]. It can be therefore expected that more functionally diverse and more functionally redundant communities would experience lower change in performance (e.g. lower mortality, lower biomass decrease) with changes in environmental conditions (e.g. ΔMCWD, ΔVPD). In our study we observed that the functional diversity levels are not significantly related to the taxonomic diversity found in the study sites across the tropics but that functional redundancy tends to be, especially for redundancy in morphological/structure and foliar nutrients traits. This points to the role of taxonomic diversity on the possible resilience of tropical ecosystems. We show that forest communities located in areas with lower soil and atmospheric water stress are generally more functionally diverse and more functionally redundant in morphological/structural, nutrients and photosynthetic traits than communities in drier areas. Such higher functional diversity and higher functional redundancy may be one reason why such forests have experienced weaker compositional and ecosystem functioning changes (e.g. carbon capture) as a result of a drying climate in comparison to forests in drier areas, as shown for forests across water availability gradients in West Africa [31, 32] and the Amazon [24, 33]. The higher functional diversity in these wetter forests can be the result of their high water availability (low MCWD and VPD, Table S2) [42, 43]. These conditions facilitate the adaptation, by means of a varied species morphology and structure [44], to a diverse set of light and moisture conditions under and at the canopy. Overall, our results support our expectation of lower functional diversity in the sites with lower long-term water availability, and are in agreement with what has been recently found not only for functional diversity but also for taxonomic and phylogenetic diversity in some local forests [31, 45]. Higher diversity and higher redundancy in functional traits may enhance ecosystem functioning, such as the ability of plant communities for carbon capture [46, 47], and thus show smaller reductions in biomass and lower mortality [48] under changes in climatic conditions. Our results are consistent with recent studies carried out in temperate forests [47] and with few tree taxa [25], which suggest a positive functional diversity-productivity relationship.

Tropical forests that experienced the largest decreases in soil water availability across the last half century, which corresponds to intermediate to high long-term average MCWD (e.g. some forests in Panama, Peru and southern Mexico), tend to have high morphology/structure and nutrients FD and FRed and high photosynthetic FD. The high functional diversity and high functional redundancy potentially points to the capabilities of such forests to better withstand the effects of a drying environment than other locations with low FD and FRed levels. Our findings show that atmospheric water availability (VPD) and its changes in the last decades mediate the FD and FRed levels across tropical forest ecosystems. Forests that experienced larger decreases in VPD over the last half century tend to be functionally redundant in morphological and nutrients traits even with increases in soil water availability (here the MCWD). However, such forests are not necessarily redundant in photosynthesis traits. One explanation for this pattern of higher redundancy of forests that experienced larger increases in MCWD and VPD is that such increases in water stress occurred in a variety of forests which are located all across the long-term mean MCWD and VPD spectrum (See Table S2). That means that these forests may well be composed of species with a wide range of functional adaptations to local conditions, adaptations that could have a possible mechanistic link via leaf phenology [49], some adapted to long periods of droughts but also others adapted to high water availability across the year. As tropical forests that increased the most in soil and atmospheric water availability are located across the long-term water availability gradient, these forests might be composed of species that have evolved with different leaf strategies ranging from evergreen to sclerophyllous and deciduous [20]. Leaf adaptations to different environments may thus also explain the pattern of increasing diversity and redundancy of leaf nutrients and photosynthesis traits in these forests that experienced larger decreases in water availability. An important further step in future analyses will be to include as much information as possible not only on the changes in climate but also on the contemporary changes in functional diversity and functional redundancy. This would allow establishing a more direct link between the effects of a changing climate on forest functioning. Moreover, while our study showed clear relations with proxies of water availability at a pantropical scale (MCWD and VPD), other environmental variables at fine scale including local topography and ground water availability may also contribute for determining local FD and FRed levels.

Forests with larger functional diversity and larger functional redundancy pools may be more resilient to further climate change. Extreme El Niño events bring about higher temperatures and droughts across tropical regions which can impact the establishment, survival and persistence of tropical forest vegetation, thus also impacting their functioning [37]. The 2015-2016 El Niño event did not seem to strongly reduce carbon gains in African tropical forests. Although we did not measure the functional composition of those tropical forests in Africa before and after the El Niño event, our modelling framework provides a general understanding of the functional diversity and functional redundancy of such forest given long-term climate conditions. Our results show that areas with higher long-term functional diversity and functional redundancy tended to show smaller decreases or larger increases in AGB, thus being more resilient to changes in environmental conditions caused by the 2015-2016 El Niño event. Overall, our results highlight that tropical dry forests, such as those in drier parts of Mexico, Colombia, south-eastern Amazonia and much of West Africa, which have experienced high long-term soil water and atmospheric water stress over the last half century, could be at higher risk than wetter forests of further functional declines given the projected changes in climatic conditions for the coming decades [50]. Further droughts may increase the water stress of drier tropical forests, which may already be at their climatic physiological limits, and could potentially drive them towards alternative stable states [18]. This is in agreement with recent findings for West African [31] and South American drier tropical forests [6, 49], where large and consistent changes in functional diversity [33] and functioning [6] have been observed. It has been hypothesised that low functional diversity and low functional redundancy may pinpoint areas that could be less resilient to further changes in environmental conditions [51]. Recent work in the wet tropics of Australia shows that tree growth has been reduced the most by positive anomalies in atmospheric water deficits in drier forests and for species growing faster in drier conditions than in wetter ones [35]. The net carbon sink of tropical seasonal forests has decreased by 0.13 Mg C ha^{-1} year^{-1} amounting to carbon losses of 3.4% per year, highlighting how the driest and warmest sites are experiencing the largest carbon sink declines and becoming carbon sources [6]. Moreover, the effects of a changing climate on drier tropical forest ecosystems may not only affect tree growth and survival but also strongly decrease their functional trait space available, possibly also affecting their functioning [49]. Both the species-level and forest-level differential demographic sensitivities to a drying climate support this hypothesis of potentially less resilience in already-drier environments. We also highlight the need for measuring more widely other plant functional traits that have a more direct link to the availability, accessibility and transport of water resources such as plant hydraulic traits (e.g. vessel density, P_{50}, hydraulic conductivity, osmotic potential, root size and depth) which are seldom available for most tropical plant species but that may shed more light into the possible responses of tropical forest to a changing climate [52, 53].

In summary, this study addresses the need to understand and monitor the responses of tropical forest ecosystems to climate change, such as the negative impacts of a drying climate on the capacity of tropical forests to sequester and store carbon. Current models of ecosystem contribution to climate mitigation lack information on earth systems feedbacks. Our results show how contemporary climate shapes the functional diversity and functional redundancy of tropical forest communities. Across the tropics climatic a diverse set of conditions support a myriad of tropical tree communities with diverse combinations of plant functional traits and different functional diversity and functional redundancy levels. Tropical communities more at risk of shifting towards alternative states could be expected to be currently the ones where lower functional diversity and redundancy is found and that are under already high water stress, such as in the drier tropical forests. From the ecosystems conservation point of view, it is of critical importance to inform decisions by mapping tropical regions in terms of their resilience to future changes in the environment. Conservation efforts need to prioritise and manage ecosystems accordingly, especially including drier tropical forests in the conservation agenda, but also considering that wet tropical forests with higher functional diversity and higher functional redundancy are likely to continue to be long term carbon stores and be more resilient in the face of climate extremes and pathogens.

Methods

Vegetation plots. We collected vegetation census data from 74 permanent vegetation plots that are part of the Global Ecosystems Monitoring network (GEM; www.gem.tropicalforests.ox.ac.uk) [54]. These plots are located in wet tropical forests, seasonally dry tropical forests, and tropical forest-savanna transitional vegetation. The sampled vegetation plots ranged in area from 0.1 to 1 ha, with most (67%) being 1 ha and only one of them being 0.1 ha (Table S2). The plots are located in Australia, Brazil, Colombia, Gabon, Ghana, Malaysian Borneo, Mexico and Peru across the four tropical continents (Table S2). In each plot, all woody plant individuals with a diameter ≥ 10 cm at breast height (DBH) or above buttress roots were measured. In the plots NXV-01 and NXV-10 in Nova Xavantina, here onwards referred to as Brazil-NX, the diameter was measured at 30 cm from the ground level as is standard in drier shorter vegetation monitoring protocols.

Plant functional traits. We directly collected plant functional trait measurements from the most abundant species that would cover at least 70% of plot basal area and that were located in most of the 74 vegetation plots mentioned above (Fig. S1; Table S1). All traits were collected following the GEM network standardised methodology across plots. Forest inventory data were used to stratify tree species by basal area dominance. The tree species that contributed most to basal area abundance were sampled with 3–5 replicate individuals per species. Eighty percent or more of basal area was often achieved in low diversity sites (e.g., montane or dry forests). For each selected tree a sun and a shade branch were sampled and in each branch 3–5 leaves were used for trait measurements. This represented a total sample of 2461 individual trees across the tropics (Fig. S1). We collected plant functional traits related to photosynthetic capacity A_{max} (µmol m^{-2} s^{-1}): light-saturated maximum rates of net photosynthesis at saturated CO_2 (2000 ppm CO_2), A_{sat} (µmol m^{-2} s^{-1}): light-saturated rates of net photosynthesis at ambient CO_2 concentration (400 ppm CO_2), R_{Dark} (µmol m^{-2} s^{-1}): dark respiration. Leaf nutrient concentration traits (%) of Ca: leaf calcium, K: leaf potassium, Mg: leaf magnesium, N: leaf nitrogen and P: leaf phosphorus. Plant morphological and structural traits, A (cm^2): leaf area, DM (g): leaf dry mass, FM (g): leaf fresh mass, LDMC (mg/g): leaf dry matter content, LWC (%): leaf water content, SLA (g/m^2): specific leaf area, T (mm): leaf thickness and WD (g/cm^3): wood density. Further details of measurements for the Peruvian Andes campaign are given in Martin et al. [55] and Enquist et al. [56], for the Malaysian campaign in Both et al. [57], and for the Ghana and Brazil campaigns in Oliveras et al. [58,], Gvozdevaite et al. [59] and for Colombia campaigns in González-M. et al. [49]. For the specific dates of plant functional traits collection see ref. [60]. For the FD and FRed calculations, as both only accept one trait value per species, from the individual level plant functional traits, we averaged the values at species level and when the species had no trait values available, we filled the gaps by averaging the trait values at the genus level. This protocol allowed us to have at least 70% of the plot's basal area covered by traits but often more. Thus, in our analysis the inclusion of plots is trait dependent in the sense that only plots with at least 70% of the BA covered by the focus trait were included in the analysis (see Table S2).

Community level functional diversity and functional redundancy

We calculated the functional diversity and functional redundancy of morphological/structural traits, leaf chemistry and photosynthetic traits, which are hypothesised to be of importance for tropical forests to respond to a drying climate (Table S1) [14, 20], based on data for species covering at least 70% of the plot basal area (Table S2) and following equations from refs. [34, 61, 62, 63]. The morphological/structural and nutrient related traits used for this analysis are A, FM, DM, LDMC, T, LWC, SLA, WD, Ca, K, Mg, N, P; and A_{sat}, A_{max} and R_{Dark} for photosynthesis. We did not build an index including all functional traits together as this would make their interpretation rather difficult as they point to different axes of the global spectrum of plant form and function[64] and also because of the difference in number of records available for each trait group. Plant functional trait diversity (FD) was calculated at the plot level using the functional dispersion metric [34], which is closely related to the RaoQ [31], and which represents the mean distance, in trait space, of each single species to the weighted centroid of all species [34]. We used the FD as it can handle any number and type of traits, because it is unaffected by species richness, it weighs the values based on the abundance of species, it is not influenced by outliers and is relatively insensitive to the effects of undersampling [65]. To calculate FD we applied the equation presented by Laliberté and Legendre [34]:

eq. 1 $$FD = \frac{\sum BA_{ip}\, z_{ip}}{\sum BA_{ip}}$$

where BA_{ip} reflects the total plot level basal area of species i in plot p and z_{ip} is the distance of species i in plot p to the weighted centroid of the n species in trait space. The plant traits were weighted by the relative basal area (in m^2) of each of the species in the plot. Therefore, FD summarises the trait diversity and represents the mean distance in trait space of each species to the centroid of all species in a given community. All numeric traits were standardised during the FD calculation.

We calculated the functional trait redundancy in the community (vegetation plots), FRed, as in Pavoine and Ricotta [62] and Ricotta et al. (*'Rstar'*) [63] and as developed in the 'uniqueness' function of the R 'adiv' package [61]. *'Rstar'* quantifies how redundant a plant community is compared to a scenario where all species would have the most distinct trait values possible. As in the case of FD, *'Rstar'* as calculated in Ricotta et al. [61, 62] works with multiple traits and takes into account species abundances. The *'Rstar'* index is complementary to the community-level functional uniqueness index *Ustar* described by Ricotta et al. [62] which is the ratio of the Rao quadratic diversity index *Q* [66, 67], that accounts for species trait dissimilarities and the Simpson index *D*, which considers the species in the community as equally and maximally dissimilar. Thus *Ustar* measures the uniqueness of the community in functional space which is obtained by including interspecies dissimilarities in the calculations of the index. *Rstar*, which is the complement of *Ustar*, represents thus a measure of community-level functional redundancy and is quantified as:

eq. 2 $$Ustar = \frac{1-D}{1-Q}$$

eq. 3 $$Rstar = 1 - Ustar$$

For an in-depth description of the functional redundancy index see refs.[61, 62, 63].

All above-mentioned analyses were carried in the R statistical environment [68] with the 'FD' and 'adiv' packages.

Climatic and soil data

In order to investigate the role that long-term climate plays on determining the community trait composition and functional diversity and redundancy across tropical forests we gathered climatic data on the potential evapotranspiration (PET in mm), precipitation accumulation (mm) and VPD (kPa) from the TerraClimate project [69] at a spatial resolution of ~4 × 4 km. The data were obtained for the period from 1958 to 2017. Using the full-term climatic dataset (1958-2017) we calculated the mean annual VPD, PET, precipitation coefficient of variation (CV; as a measure of seasonality in water availability) and the maximum climatological water deficit (MCWD). The MCWD is a metric for drought intensity and severity and is defined as the most negative value of the climatological water deficit (CWD) over each calendar year. The VPD is an indicator of plant transpiration and water loss [14]. CWD is defined as precipitation (P) (mm/month) – PET (mm/month) with a minimum deficit of 0. The MCWD was calculated as in Malhi et al.[13] where MCWD=min(CWD1…CWD12). As a final step we converted the MCWD so that positive values indicate increases in water stress. We also calculated the change in the climatic variables (ΔMCWD, ΔVPD and ΔCV) between a first period corresponding to a climatology of 30 years encompassing 1958-1987 and a second period encompassing the years 1988-2017. The climatology of 30 years to calculate the different time periods climate was selected as recommended by the World Meteorological Organization in order to characterise the average weather conditions for a given area (www.wmo.int/pages/prog/wcp/ccl/faqs.php). We also obtained soil texture (percent clay and sand) and chemistry (soil pH and cation exchange capacity, CEC) gridded data from the SoilGrids project (www.soilgrids.org) and used this as extra covariates in our modelling framework. We then tested the correlation between all pairs of climatic variables (full-term and their changes) and also between the soil variables. We observed that MCWD and CV had Pearson's correlation coefficients |>0.70| and also CEC and pH and Clay and Sand had correlation coefficients |>0.70| (Fig. S11) and we thus dropped CV and its change, Sand and pH from the analyses as to avoid distorting model coefficients in the modelling stage [70]. We then carried out a principal component analysis (PCA) using the MCWD and VPD climatic variables (average of full-term and their changes) and another with the soil variables to investigate the distribution of the vegetation plots in climate and soil space and to describe how much of this distribution can be explained by each of these. For the PCA analysis we used the ‘stats’ package in R.

Statistical analysis

Functional Diversity and Functional Redundancy statistical analysis

We investigated the variation in morphological/structural, leaf chemistry and photosynthetic FD and FRed across tropical forests by modelling their relation with mean MCWD, VPD for the period 1958-2017 and their interaction, the ΔMCWD and ΔVPD between the first and second periods and their interaction and soil chemistry (CEC) and texture (Clay%). For the photosynthesis statistical models, given their lower sample size (n=22; Table S2), interaction terms were not included and to avoid overfitting we first tested by means of leave-one-out cross-validation (LOO)[71] if the soil covariates improved or not the models with only climate information. We found soil data did not improve our models (Table S8) and thus left CEC and Clay out of the photosynthesis models. We also calculated the relative change (%) in climatic conditions but this did not improve model predictions (data not shown) and thus we only present results that include the absolute changes in MCWD and VPD. We included the change in MCWD and VPD as we wanted to understand if areas that have experienced stronger changes in climate showed lower or higher functional diversity and functional redundancy than others that have experienced milder climate changes. In the same way we included the interaction between MCWD and VPD (and also between ΔMCWD and ΔVPD) as there may be regions where high values of one of these variables may not be related to the values of the other, e.g. high MCWD may not be related to high VPD. Prior to the statistical modelling we centred and standardised (generated z-scores) all climatic and soil variables.

We tested for spatial autocorrelation effects in the FD and FRed model residuals using the Moran's I test and found a significant effect for the photosynthesis and nutrients FD models and for the FRed nutrients model (Table S9). Thus, for those data we calculated the spatial distance at which such spatial effect decreased and found that a distance of 2 km was sufficient. We then generated an ID for each group of plots (group ID) that were at most 2 km away from each other and included such group ID as a random factor in those statistical models. As some plots were smaller than 1 ha (Table S2) we included the z-scores of plot size as a covariate in all statistical models to account for its possible effect. We log transformed the FD and FRed indices to improve the normality of the data and applied linear mixed-effects models with a Gaussian error structure accounting for difference in plot size and spatial autocorrelation as described above under a Bayesian framework. The mixed-effects models were run with normal diffuse priors with mean 0 and 2.5 standard deviation to adjust the scale of coefficients and 10 standard deviations to adjust the scale of the intercept, three chains and 10000 iterations to avoid issues with model convergence. We computed the highest density intervals (HDI) rendering the range containing the 90% most probable effect values and calculated the ROPE values using such HDI as suggested in Makowski et al.[72]. The 95% HDI was not used as this range has been shown to be unstable with ESS < 10,000 (effective sample size)[73]. We considered a climatic variable had an important (significant) effect on the response variable if the 90% HDI did not overlap 0. Posterior density distributions for all models and covariates included in the models are shown in Fig. S12 and Fig. S13.

Based on the statistical models described above we created spatial predictions of Functional Diversity (FD) and Functional Redundancy (FRed) at a pantropical scale. We defined the 'low', 'intermediate' and 'high' FD and FRed groups by defining the range in FD and FRed values and dividing that range between three in order to allocate the FD and FRed predicted values to each of these groups and be able to state what is the predicted percent area of tropical and subtropical dry and moist broadleaf forests with low, medium and high FD and FRed. We also tested the robustness of the spatial predictions of FD and FRed by also developing the models by leaving out the data from one continent (South East Asia and Australia together), fitting the model again, and comparing the resulting spatial predictions to the full model prediction maps by means of Spearman correlations. In Fig. S14 we also highlight locations across the tropics with climate and soil conditions outside of our climatic and soil calibration space, thus not covered by the range in our sampling locations, which may represent locations where our models are extrapolating the relationships found.

Relations between Functional Diversity, Functional Redundancy and Aboveground biomass

We obtained the above ground biomass data (AGB) from an independent set of 100 vegetation plots in Africa before (AGB_{pre}) and after (AGB_{post}) the 2015 El Niño event from Bennett et al. [37] . The plots from Bennet et al. include censuses from 2000 onward where the median plot size is 1 ha, the mean initial census was May 2008, with the mean pre-El Niño census in April 2014, and mean post-El Niño census in February 2017. The plots have a mean monitoring length pre-El Niño of 8.3 years, with a mean length of the El Niño interval being 2.7 years. To calculate AGB Bennet et al. [37] used the BiomasaFP R package, including the calculation of the census interval corrections for AGB where Pre-El Niño means of these variables are time weighted using the census interval lengths. For a full description of the AGB data see Bennett et al. [37]. We calculated the ΔAGB as:

eq. 4 $\Delta AGB = (AGB_{post} - AGB_{pre})$

Before modelling we eliminated statistical outliers in the AGB values, this is values more than 1.5 the interquartile range above the third quartile or below the first quartile. We therefore only used 86 plots in our analysis. We modelled the ΔAGB as a function of the predicted (see methods above) FD and FRed maps scores from each functional group (morphology/structure, nutrients and photosynthesis; Fig. 3 and Fig. 4), one model was built per functional group. Each model included the FD and FRed index (e.g. FD and FRed of nutrients) and their interaction with ΔMCWD and ΔVPD as to test the effect of a changing climate on the effects of FD and FRed on above ground biomass change. We accounted for plot size by including as a covariate in the models and used a Gaussian error structure model under a Bayesian framework. The ΔAGB statistical models were run with normal diffuse priors with three chains and 5000 iterations.

We carried out all statistical analysis in the R statistical environment [68] using the, 'rstanarm', 'loo', 'bayestestR', 'egg' and 'BEST' packages.

Data availability

The vegetation census and plant functional traits data that support the findings of this study are available from their sources (www.ForestPlots.net and gem.tropicalforests.ox.ac.uk/). The processed community-level data used in this study will be made available in a public repository.

Code availability

The main R code used in this study will be deposited in a public repository and can be accessed through the principal investigator upon request.

References

1. Barlow, J. *et al*. Anthropogenic disturbance in tropical forests can double biodiversity loss from deforestation. *Nature* **535**, 144-147 (2016).

2. Beech, E., Rivers, M., Oldfield, S. & Smith, P. P. GlobalTreeSearch: The first complete global database of tree species and country distributions. *J. Sustainable For.* **36**, 454-489 (2017).

3. ter Steege, H. *et al*. The discovery of the Amazonian tree flora with an updated checklist of all known tree taxa. *Scientific reports* **6**, 29549 (2016).

4. Hubau, W. *et al*. Asynchronous carbon sink saturation in African and Amazonian tropical forests. *Nature* **579**, 80-87 (2020).

5. Pan, Y. *et al*. A large and persistent carbon sink in the world's forests. *Science* **333**, 988-993 (2011).

6. Maia, V. A. *et al*. The carbon sink of tropical seasonal forests in southeastern Brazil can be under threat. *Science Advances* **6**, eabd4548 (2020).

7. Malhi, Y. *et al*. The regional variation of aboveground live biomass in old-growth Amazonian forests. *Global Change Biol.* **12**, 1107-1138 (2006).

8. Phillips, O. L. *et al*. Drought sensitivity of the Amazon rainforest. *Science* **323**, 1344-1347 (2009).

9. Malhi, Y. *et al*. Climate change, deforestation, and the fate of the Amazon. *Science* **319**, 169-172 (2008).

10. Gatti, L. V. *et al*. Amazonia as a carbon source linked to deforestation and climate change. *Nature* **595**, 388-393 (2021).

11. Hisano, M., Searle, E. B. & Chen, H. Y. Biodiversity as a solution to mitigate climate change impacts on the functioning of forest ecosystems. *Biological Reviews* **93**, 439-456 (2018).

12. Pecl, G. T. *et al*. Biodiversity redistribution under climate change: Impacts on ecosystems and human well-being. *Science* **355** (2017).

13. Malhi, Y. *et al*. Exploring the likelihood and mechanism of a climate-change-induced dieback of the Amazon rainforest. *Proc. Natl. Acad. Sci. U. S. A.* **106**, 20610-20615 (2009).

14. Seager, R. *et al*. Climatology, variability, and trends in the US vapor pressure deficit, an important fire-related meteorological quantity. *Journal of Applied Meteorology and Climatology* **54**, 1121-1141 (2015).

15. Smith, M. N. *et al*. Empirical evidence for resilience of tropical forest photosynthesis in a warmer world. *Nature Plants* **6**, 1225-1230 (2020).

16. Yuan, W. *et al*. Increased atmospheric vapor pressure deficit reduces global vegetation growth. *Science advances* **5**, eaax1396 (2019).

17. Brodribb, T. J., Powers, J., Cochard, H. & Choat, B. Hanging by a thread? Forests and drought. *Science* **368**, 261-266 (2020).

18. Allen, K. *et al*. Will seasonally dry tropical forests be sensitive or resistant to future changes in rainfall regimes? *Environmental Research Letters* **12**, 023001 (2017).

19. Esquivel-Muelbert, A. *et al*. Compositional response of Amazon forests to climate change. *Global Change Biol.* **25**, 39-56 (2019).

20. Aguirre-Gutiérrez, J. *et al*. Drier tropical forests are susceptible to functional changes in response to a long-term drought. *Ecol. Lett.* **22**, 855-865 (2019).

21. Cadotte, Marc W., Kelly Carscadden, and Nicholas Mirotchnick. "Beyond species: functional diversity and the maintenance of ecological processes and services." Journal of applied ecology 48.5 (2011): 1079-1087.

22. Aguirre-Gutiérrez, J., *et al.* Butterflies show different functional and species diversity in relationship to vegetation structure and land use. Global Ecology and Biogeography **26**: 1126-1137 (2017).

23. Arruda Almeida, B., *et al.* Comparing species richness, functional diversity and functional composition of waterbird communities along environmental gradients in the neotropics. *PloS One* 13.7: e0200959 (2018).

24. Yachi, S. & Loreau, M. Biodiversity and ecosystem productivity in a fluctuating environment: the insurance hypothesis. *Proceedings of the National Academy of Sciences* **96**, 1463-1468 (1999).

25. Correia, D. L. P., Raulier, F., Bouchard, M. & Filotas, É. Response diversity, functional redundancy, and post-logging productivity in northern temperate and boreal forests. *Ecol. Appl.* **28**, 1282-1291 (2018).

26. Elmqvist, T. *et al*. Response diversity, ecosystem change, and resilience. *Frontiers in Ecology and the Environment* **1**, 488-494 (2003).

27. Loreau, Michel, and Claire De M. Biodiversity and ecosystem stability: a synthesis of underlying mechanisms. *Ecol. Lett.* 16: 106-115 (2013).

28. Petchey, O. L., Evans, K. L., Fishburn, I. S. & Gaston, K. J. Low functional diversity and no redundancy in British avian assemblages. *J. Anim. Ecol.* **76**, 977-985 (2007).

29. Jucker, T., *et al.* Stabilizing effects of diversity on aboveground wood production in forest ecosystems: linking patterns and processes. *Ecol. Lett.* 17.12: 1560-1569 (2014).

30. Fonseca, C. R. & Ganade, G. Species functional redundancy, random extinctions and the stability of ecosystems. *J. Ecol.*, 118-125 (2001).

31. Aguirre-Gutiérrez, J. *et al*. Long-term droughts may drive drier tropical forests towards increased functional, taxonomic and phylogenetic homogeneity. *Nature communications* **11**, 1-10 (2020).

32. Fauset, S. *et al*. Drought-induced shifts in the floristic and functional composition of tropical forests in Ghana. *Ecol. Lett.* **15**, 1120-1129 (2012).

33. Esquivel-Muelbert, A., Baker, T. R., Dexter, K. G., Lewis, S. L. & et al. Compositional response of Amazon forests to climate change. *Global Change Biology* **25,** 39-56 (2019).

34. Laliberté, E. & Legendre, P. A distance-based framework for measuring functional diversity from multiple traits. *Ecology* **91**, 299-305 (2010).

35. Bauman, D. *et. al.* Tropical tree growth sensitivity to climate is driven by species intrinsic growth rate and leaf traits. *Global Change Biology, In press* (2021).

36. Quesada, C. et al. Basin-wide variations in Amazon forest structure and function are mediated by both soils and climate. *Biogeosciences* **9**, 2203–2246 (2012).

37. Bennett, A. C. *et al*. Resistance of African tropical forests to an extreme climate anomaly. *Proceedings of the National Academy of Sciences* **118** (2021).

38. Shukla, P. R. *et al*. IPCC, 2019: Climate Change and Land: an IPCC special report on climate change, desertification, land degradation, sustainable land management, food security, and greenhouse gas fluxes in terrestrial ecosystems. (2019).

39. Ashton, I. W., Miller, A. E., Bowman, W. D. & Suding, K. N. Niche complementarity due to plasticity in resource use: plant partitioning of chemical N forms. *Ecology* **91**, 3252-3260 (2010).

40. Petchey, O. L. On the statistical significance of functional diversity effects. *Funct. Ecol.*, 297-303 (2004).

41. Bruno, J. F., Stachowicz, J. J. & Bertness, M. D. Inclusion of facilitation into ecological theory. *Trends in ecology & evolution* **18**, 119-125 (2003).

42. ter Steege, H. *et al*. Continental-scale patterns of canopy tree composition and function across Amazonia. *Nature* **443**, 444-447 (2006).

43. Raes, N., Roos, M. C., Slik, J. W. F., Van Loon E. Emiel & Steege, H. T. Botanical richness and endemicity patterns of Borneo derived from species distribution models. *Ecography* **32**, 180-192 (2009).

44. Shenkin, A. *et al*. The Influence of Ecosystem and Phylogeny on Tropical Tree Crown Size and Shape. *Front. For. Glob. Change* **3** (2020).

45. Harrison, S., Spasojevic, M. J. & Li, D. Climate and plant community diversity in space and time. *Proceedings of the National Academy of Sciences* **117**, 4464-4470 (2020).

46. Grossman, J. J., Cavender-Bares, J., Hobbie, S. E., Reich, P. B. & Montgomery, R. A. Species richness and traits predict overyielding in stem growth in an early-successional tree diversity experiment. *Ecology* **98**, 2601-2614 (2017).

47. Williams, L. J. *et al*. Remote spectral detection of biodiversity effects on forest biomass. *Nature Ecology & Evolution* **5**, 46-54 (2021).

48. Hutchison, C., Gravel, D., Guichard, F. & Potvin, C. Effect of diversity on growth, mortality, and loss of resilience to extreme climate events in a tropical planted forest experiment. *Scientific reports* **8**, 1-10 (2018).

49. González-M, R. *et al*. Diverging functional strategies but high sensitivity to an extreme drought in tropical dry forests. *Ecol. Lett.* (2021).

50. Hoegh-Guldberg, O. *et al*. Impacts of 1.5 C global warming on natural and human systems. *Global warming of 1.5 C.An IPCC Special Report* (2018).

51. de la Riva, Enrique G *et al*. The importance of functional diversity in the stability of Mediterranean shrubland communities after the impact of extreme climatic events. *Journal of Plant Ecology* **10**, 281-293 (2017).

54. Malhi, Y. *et al*. The Global Ecosystems Monitoring network: Monitoring ecosystem productivity and carbon cycling across the tropics. *Biol. Conserv.* **253**, 108889 (2021).

55. Martin, R. E. *et al*. Covariance of Sun and Shade Leaf Traits Along a Tropical Forest Elevation Gradient. *Frontiers in plant science* **10**, 1810 (2020).

56. Enquist, B. J. *et al*. Assessing trait-based scaling theory in tropical forests spanning a broad temperature gradient. *Global Ecol. Biogeogr.* **26**, 1357-1373 (2017).

57. Both, S. *et al*. Logging and soil nutrients independently explain plant trait expression in tropical forests. *New Phytol.* **221**, 1853-1865 (2019).

58. Oliveras, I. *et al*. The influence of taxonomy and environment on leaf trait variation along tropical abiotic gradients. *Frontiers in Forests and Global Change* **3**, 18 (2020).

59. Gvozdevaite, A. *et al*. Leaf-level photosynthetic capacity dynamics in relation to soil and foliar nutrients

along forest–savanna boundaries in Ghana and Brazil. *Tree Physiol.* **38**, 1912-1925 (2018).

60. Aguirre-Gutiérrez, J. *et al*. Pantropical modelling of canopy functional traits using Sentinel-2 remote sensing data. *Remote Sens. Environ.* **252**, 112122 (2021).

61. Pavoine, S. adiv: An r package to analyse biodiversity in ecology. *Methods in Ecology and Evolution* **11**, 1106-1112 (2020).

62. Pavoine, S. & Ricotta, C. A simple translation from indices of species diversity to indices of phylogenetic diversity. *Ecol. Ind.* **101**, 552-561 (2019).

63. Ricotta, C. *et al*. Measuring the functional redundancy of biological communities: a quantitative guide. *Methods in Ecology and Evolution* **7**, 1386-1395 (2016).

64. Díaz, Sandra, Jens Kattge, Johannes HC Cornelissen, Ian J. Wright, Sandra Lavorel, Stéphane Dray, Björn Reu et al. The global spectrum of plant form and function. *Nature* 529, no. 7585 (2016): 167-171.

65. van der Plas, F., Van Klink, R., Manning, P., Olff, H. & Fischer, M. Sensitivity of functional diversity metrics to sampling intensity. *Methods in Ecology and Evolution* **8**, 1072-1080 (2017).

66. Rao, C. R. Diversity and dissimilarity coefficients: a unified approach. *Theor. Popul. Biol.* **21**, 24-43 (1982).

67. Simpson, E. H. Measurement of diversity. *Nature* (1949).

68. R Core Team. R: A language and environment for statistical computing. R Foundation for Statistical Computing, Vienna, Austria. Available online at https://www.R-project.org/. **3.4.1** (2019).

69. Abatzoglou, J. T., Dobrowski, S. Z., Parks, S. A. & Hegewisch, K. C. TerraClimate, a high-resolution global dataset of monthly climate and climatic water balance from 1958–2015. *Scientific data* **5**, 170191 (2018).

70. Dormann, C. F. *et al*. Collinearity: a review of methods to deal with it and a simulation study evaluating their performance. *Ecography* **36**, 27-46 (2013).

71. Vehtari, A., Gelman, A. & Gabry, J. Practical Bayesian model evaluation using leave-one-out cross-validation and WAIC. *Statistics and Computing* **27**, 1413-1432 (2017).

72. Makowski, D., Ben-Shachar, M. S. & Lüdecke, D. bayestestR: Describing effects and their uncertainty, existence and significance within the Bayesian framework. *Journal of Open Source Software* **4**, 1541 (2019).

73. Kruschke, J. K. in *Doing Bayesian data analysis: A tutorial with R, JAGS, and Stan* (Academic Press, 2014).

Supplementary Information

Supplementary figures S1 to S15

Functional susceptibility of tropical forests to climate change

Jesús Aguirre-Gutiérrez et al.

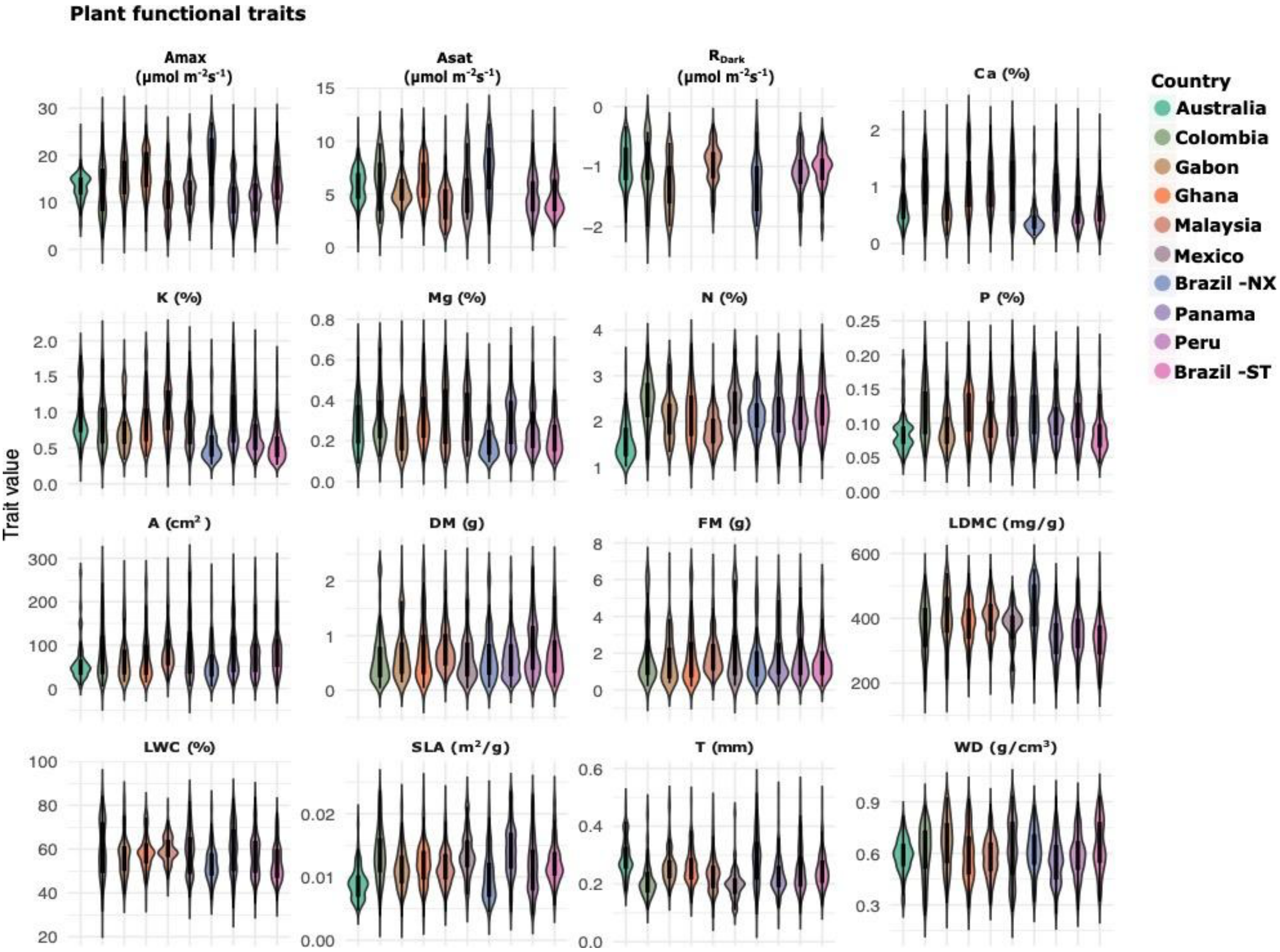

Figure S1. Violin plots of the plant functional traits and their value ranges across the study area. Plant functional trait values for all functional traits included in the analyses are shown. The plant functional traits used in the study with raw trait values are shown but these data were log-transformed prior to further analysis. The colours correspond to the field sampling areas where in situ traits collection plots are located; the Y axis shows the raw data values for each functional trait. Photosynthetic traits are A_{max}: Light-saturated maximum rates of net photosynthesis at saturated CO_2 (2000 ppm CO_2); µmol m^{-2} s^{-1}), A_{sat}: light-saturated rates of net photosynthesis at ambient CO_2 concentration (400 ppm CO_2; µmol m^{-2} s^{-1}), R_{Dark}: dark respiration (µmol m^{-2} s^{-1}). Leaf nutrient concentration traits are, Ca: leaf calcium (%), K: leaf potassium (%), Mg: leaf magnesium (%), N: leaf nitrogen (%), P: leaf phosphorus (%). Leaf morphological and structural traits are, A: leaf area (cm²), DM: leaf dry mass (g), FM: leaf fresh mass (g), LDMC: leaf dry matter content (mg/g), LWC: leaf water content (%), SLA: specific leaf area (m2/g), T: leaf thickness (mm), WD: wood density (g/cm^3). No traits were collected in Mexico and were thus assigned to the vegetation censuses from other locations as explained in the methods section. Brazil -ST: Brazil Santarem, Brazil -NX: Brazil Nova Xavantina.

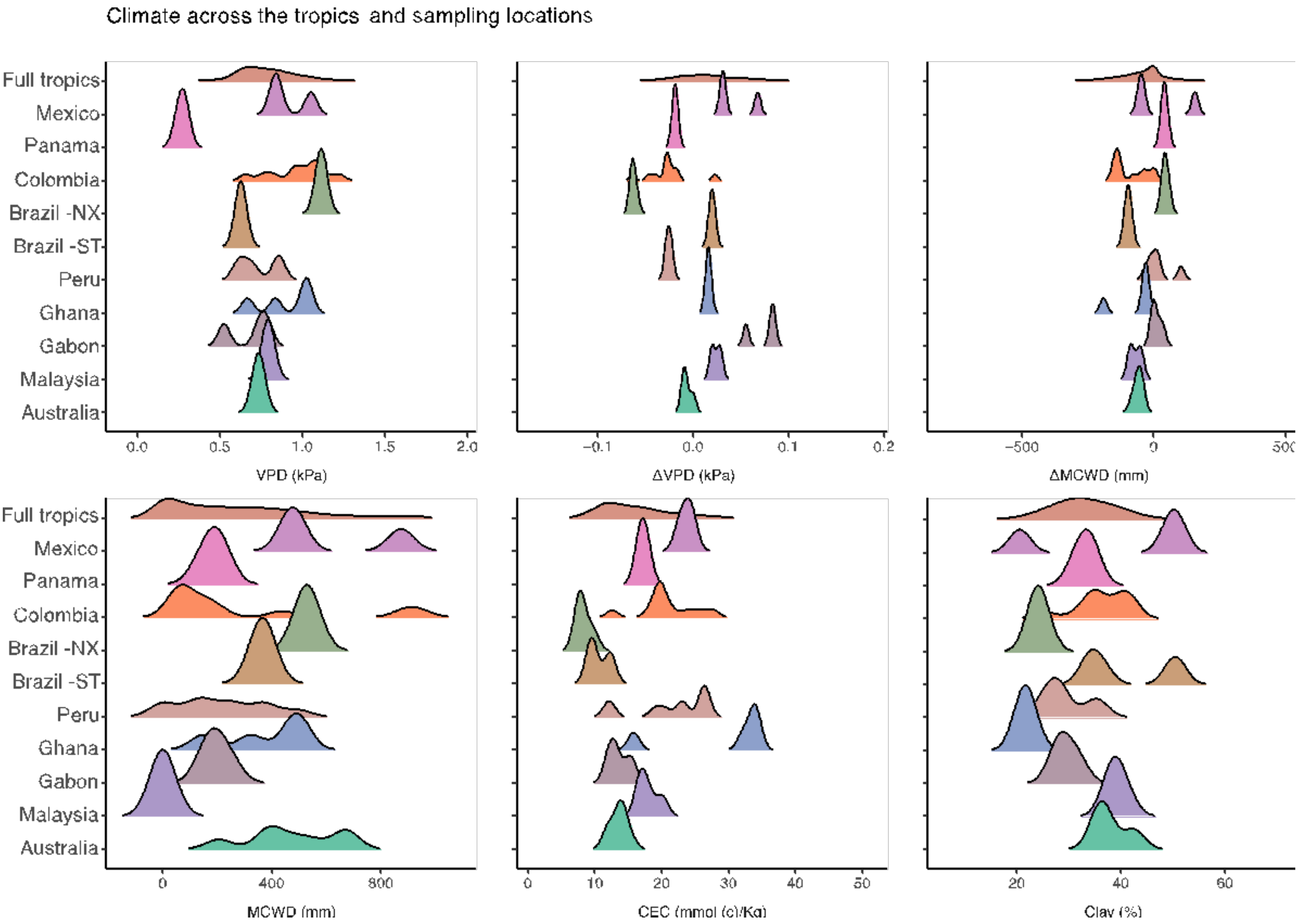

Figure S2. Density plots of the climatic and soil conditions that encompass each field sampling location where plant functional traits and vegetation censuses were collected. The top density graph of each climatic and soil variable shows the values found across the tropical and subtropical dry and moist broadleaf forests. VPD: vapour pressure deficit, MCWD: maximum climatic water deficit, CEC: cation exchange capacity, Δ: change.

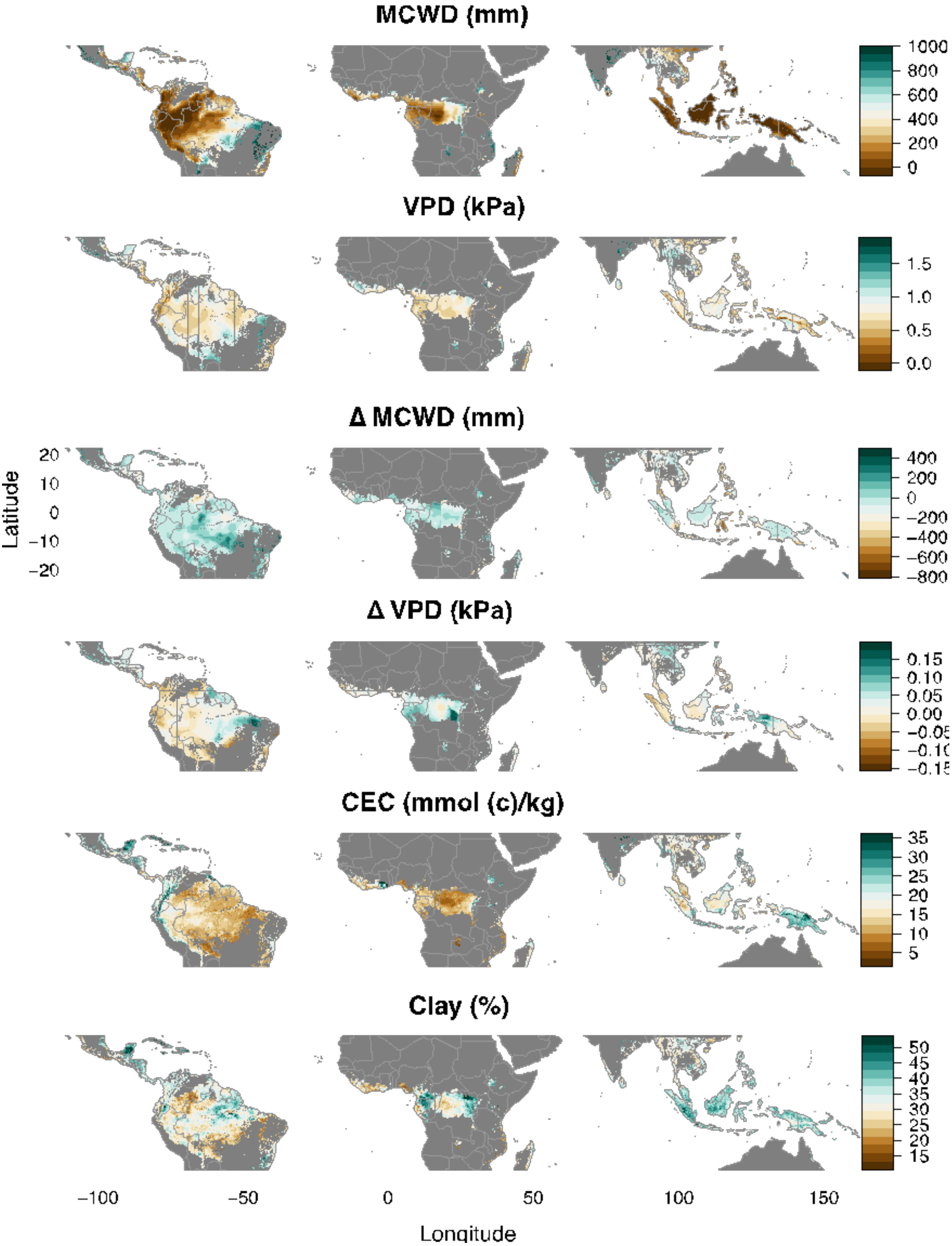

Figure S3. Spatial distribution of climatic and soil conditions across the tropical and subtropical dry and moist broadleaf forests. MCWD: maximum climatic water deficit, VPD: vapour pressure deficit, CEC: soil cation exchange capacity, Clay: soil clay content. Δ: change.

a) PCA of sampling locations in climate space

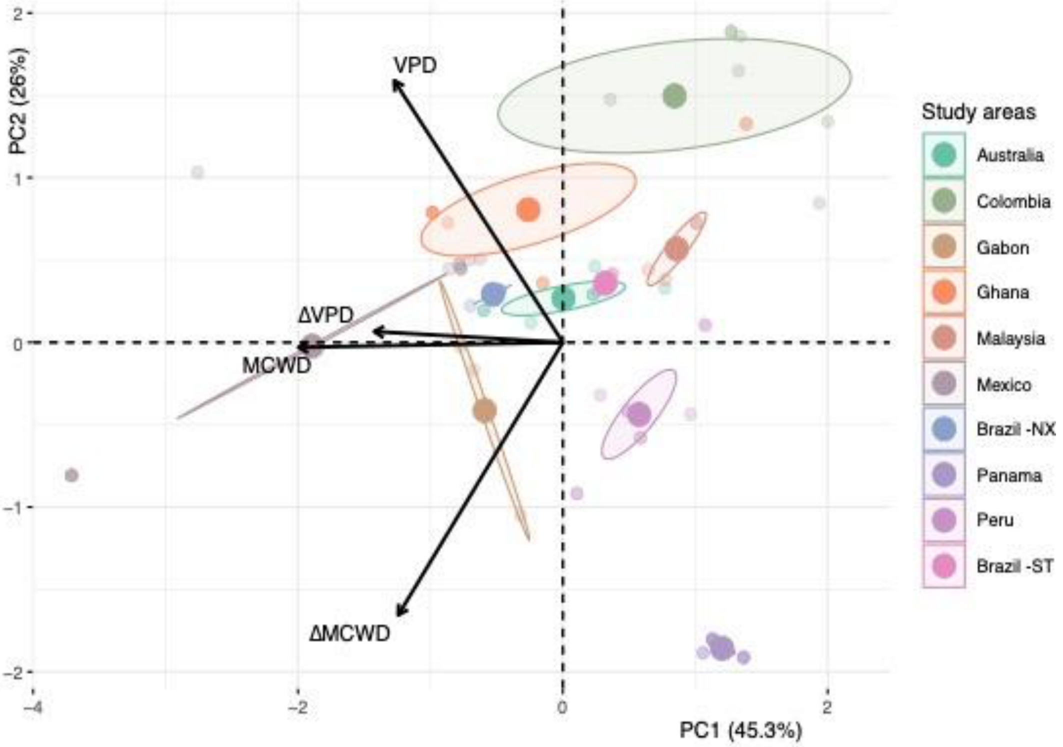

b) PCA of sampling locations according to soil characteristics

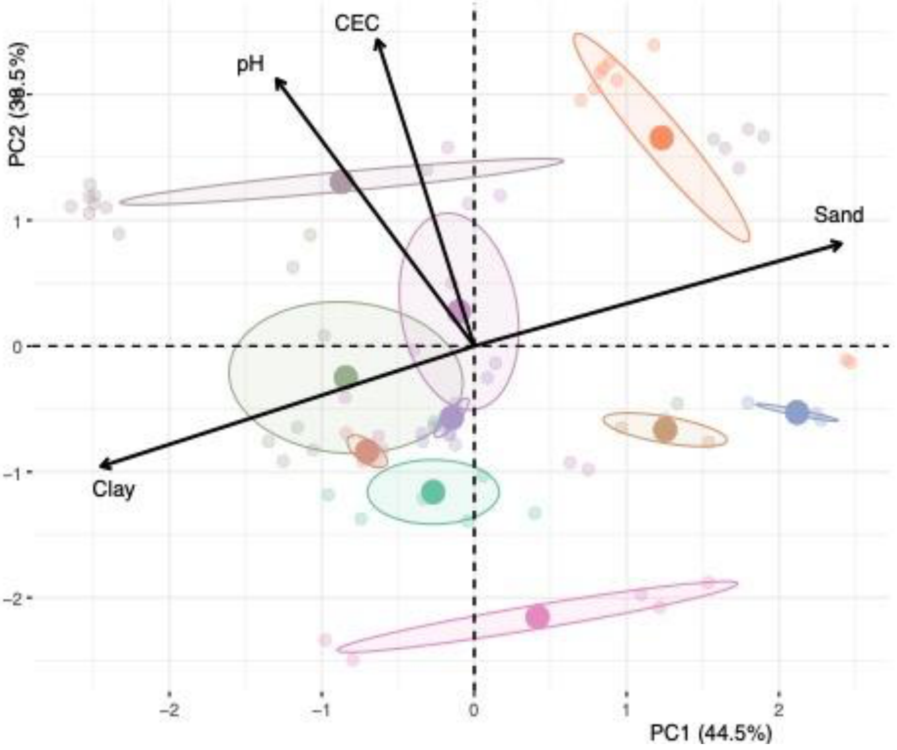

Figure S4 Principal component analysis of the distribution of the plot locations in climatic (a) and soil (b) space. MCWD: average Maximum Climatic Water Deficit and VPD: average Vapour Pressure Deficit, ΔMCWD and ΔVPD: change in MCWD and VPD respectively between the 1958-1987 and 1988-2017 period. MCWD and VPD represent the full-term climatic conditions (1958-2017 period). CEC: cation exchange capacity and soil pH are highly correlated and only CEC is used for further analysis. Clay and sand are highly correlated and only clay is used for further analysis. Coloured ellipsoids in a) and b) encompass 95% of the distribution of the vegetation plots from each field sampling location.

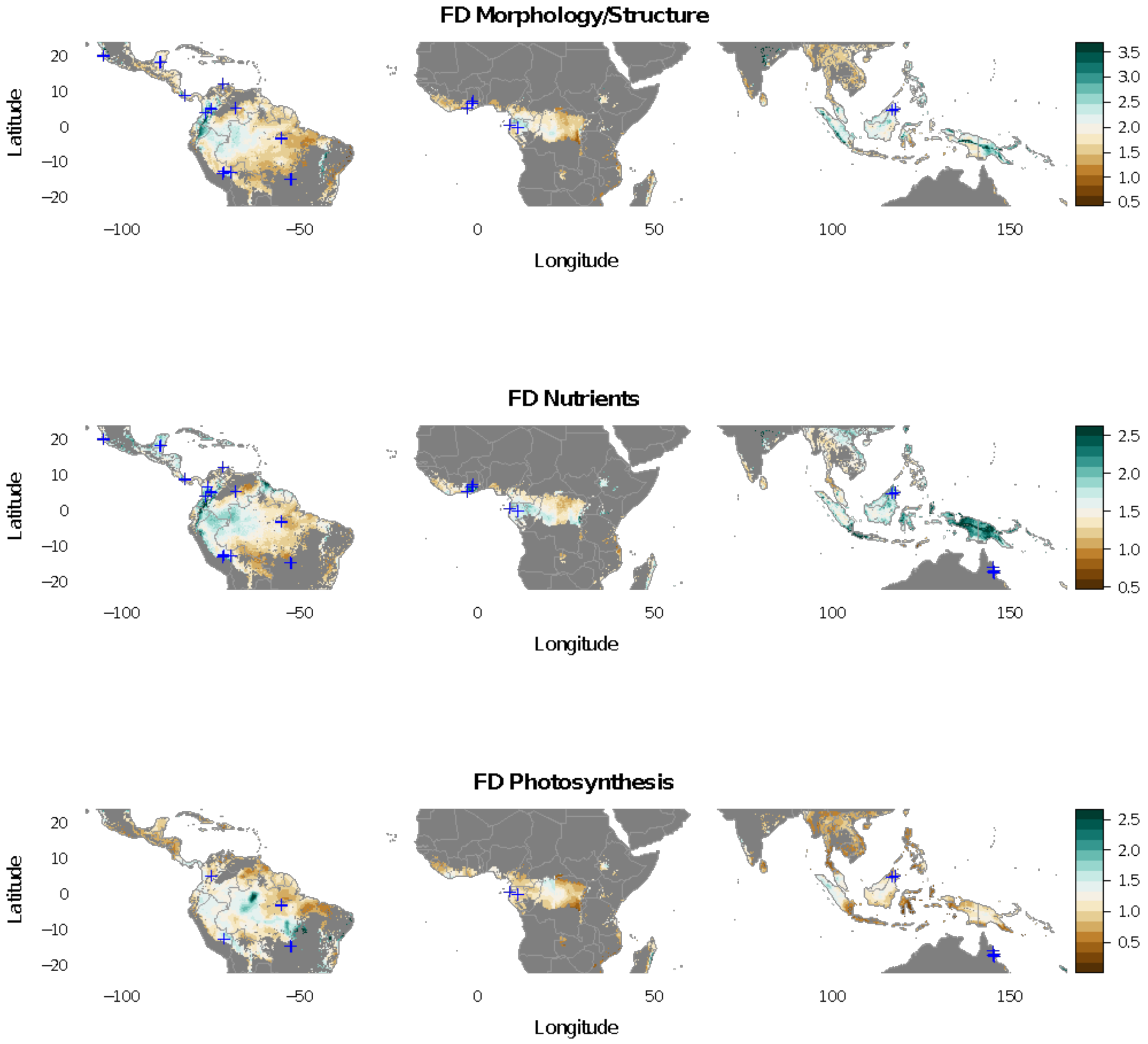

Figure S5. Spatial predictions of functional diversity (FD) depicting the locations of vegetation plots (blue crosses) that were used to fit the statistical models of morphological/structural (top panel), nutrients (middle panel) and photosynthetic (bottom panel) traits. For details about the plots, their location and climatic and soil conditions see Table S1).

FRed Morphology/Structure

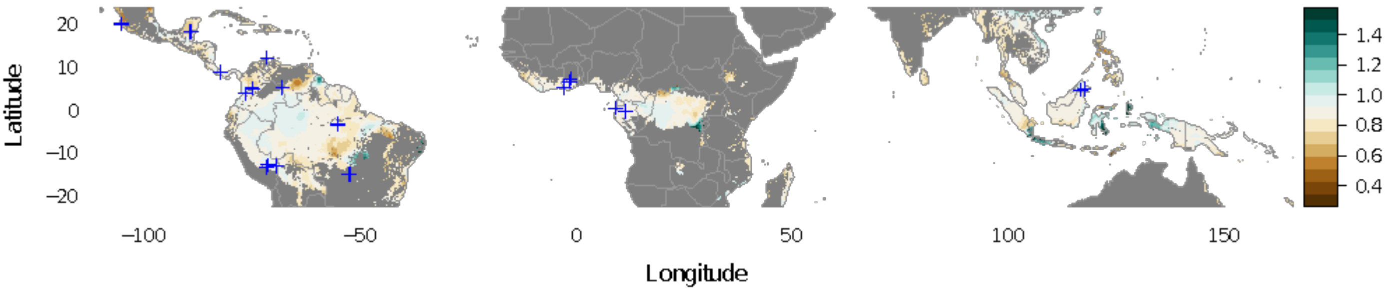

FRed Nutrients

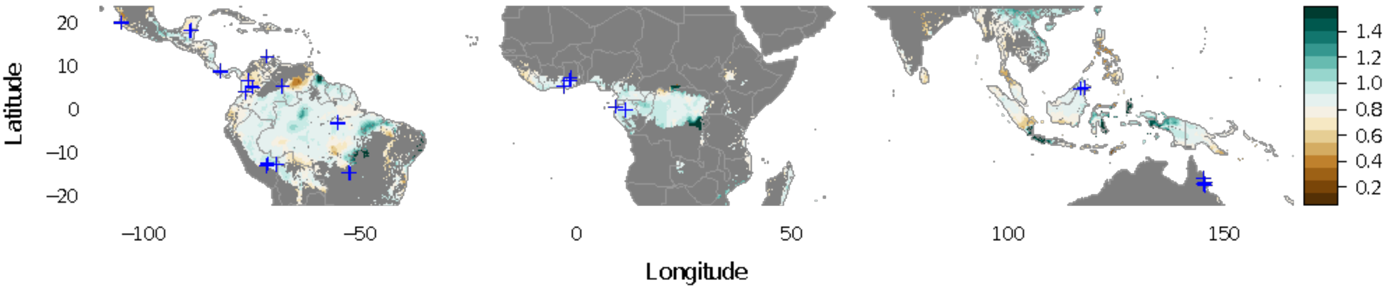

FRed Photosynthesis

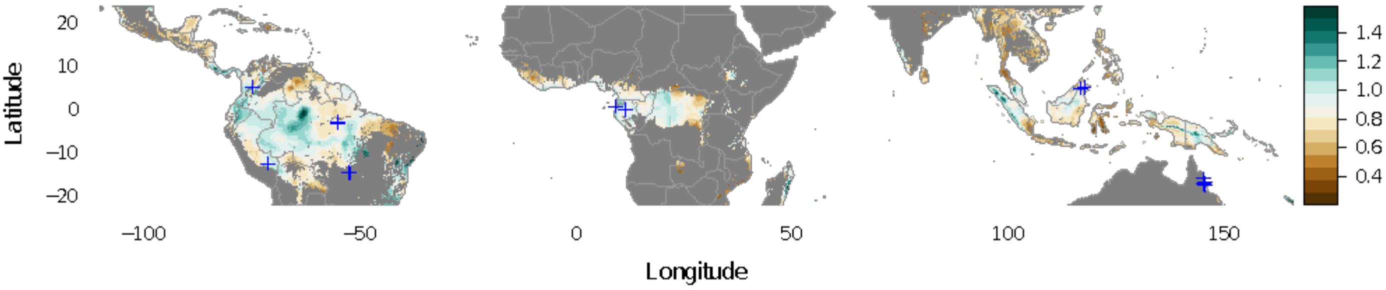

Figure S6. Spatial predictions of functional redundancy (FRed) depicting the locations of vegetation plots (blue crosses) that were used to fit the statistical models of morphological/structural (top panel), nutrients (middle panel) and photosynthetic (bottom panel) traits. For details about the plots, their location and climatic and soil conditions see Table S1).

FD –Morphology/Structure Full Model

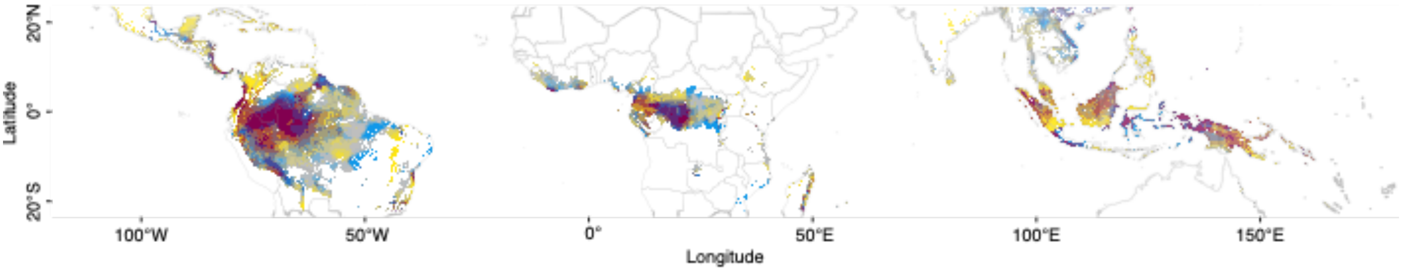

FD –Morphology/Structure Americas out

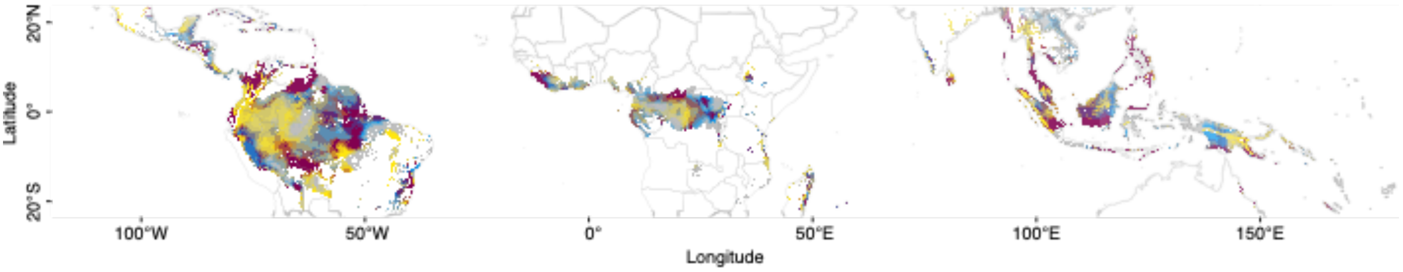

FD –Morphology/Structure Africa out

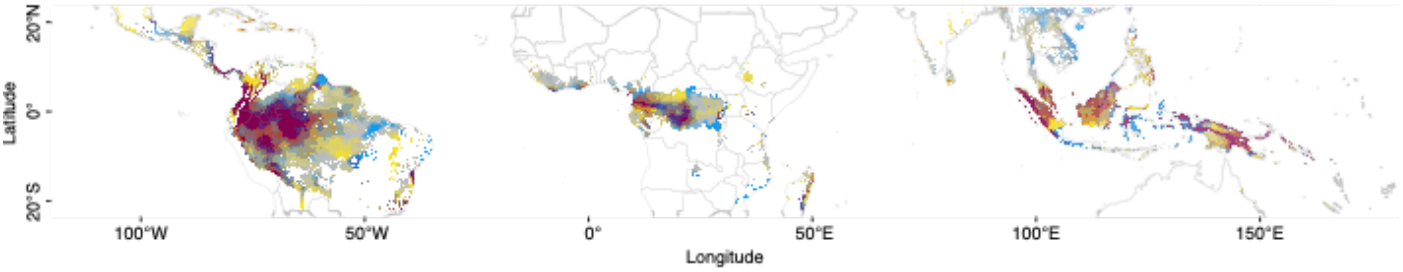

FD –Morphology/Structure Asia out

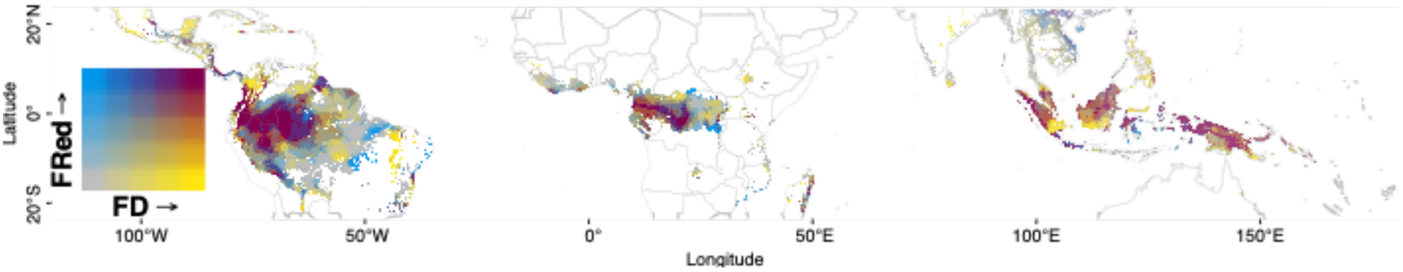

Figure S7. Bivariate maps combining the functional diversity (FD) and redundancy (FRed) for the morphological traits. Each map shows the predictions obtained using the full dataset (full model, top panel) and the changes that occur by leaving the plots from each continent out of the model. The second panel shows the spatial predictions when leaving the records from the Americas out of model fitting, the third panel when leaving records from Africa out and the bottom panel when leaving the records from Asia and Australia out from model fitting.

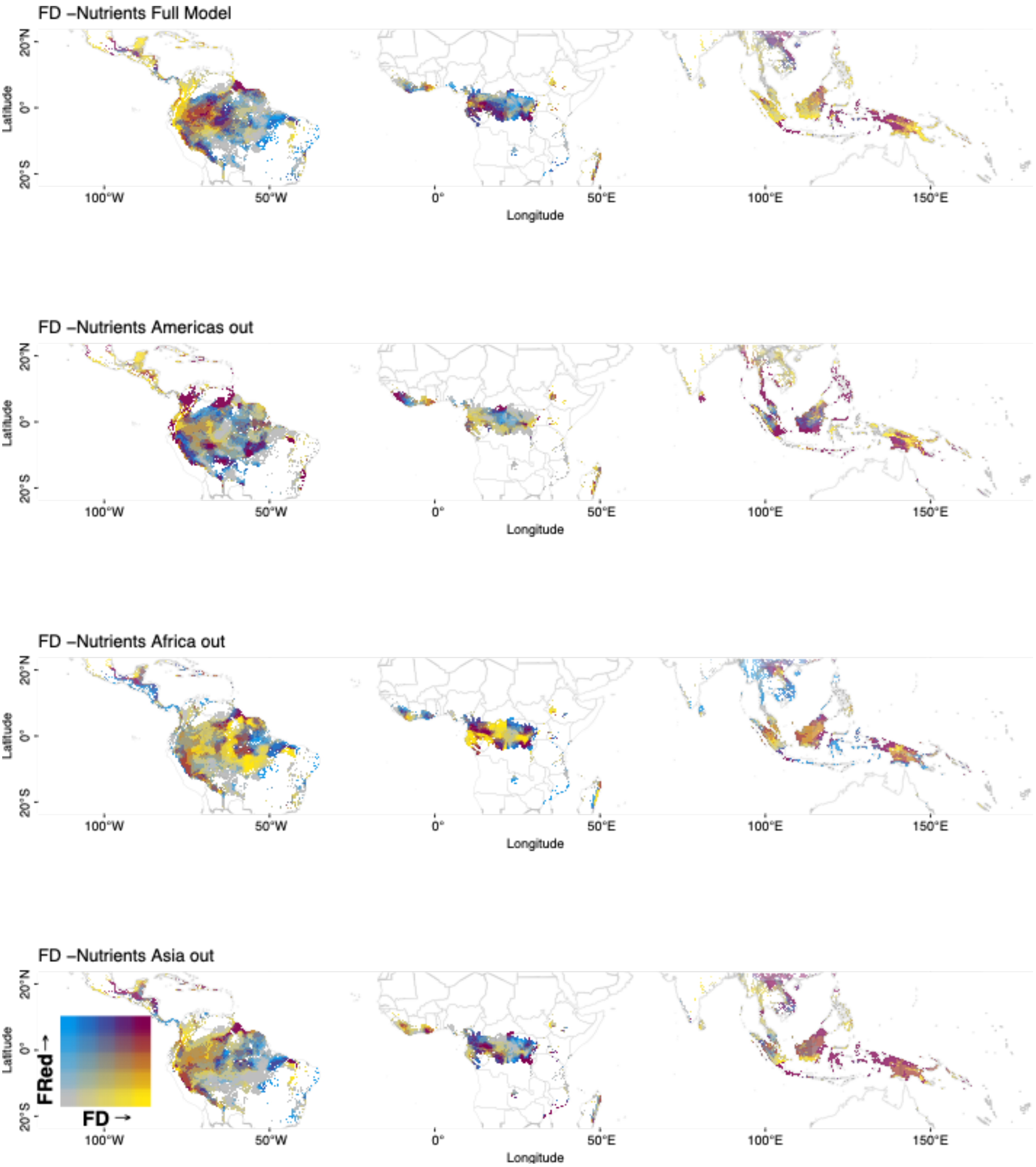

Figure S8. Bivariate maps combining the functional diversity (FD) and redundancy (FRed) for the nutrients traits. Each map shows the predictions obtained using the full dataset (Full model) and the changes that occur by leaving the plots from each continent out of the model. The second panel shows the spatial predictions when leaving the records from the Americas out of model fitting, the third panel when leaving records from Africa out and the bottom panel when leaving the records from Asia and Australia out from model fitting.

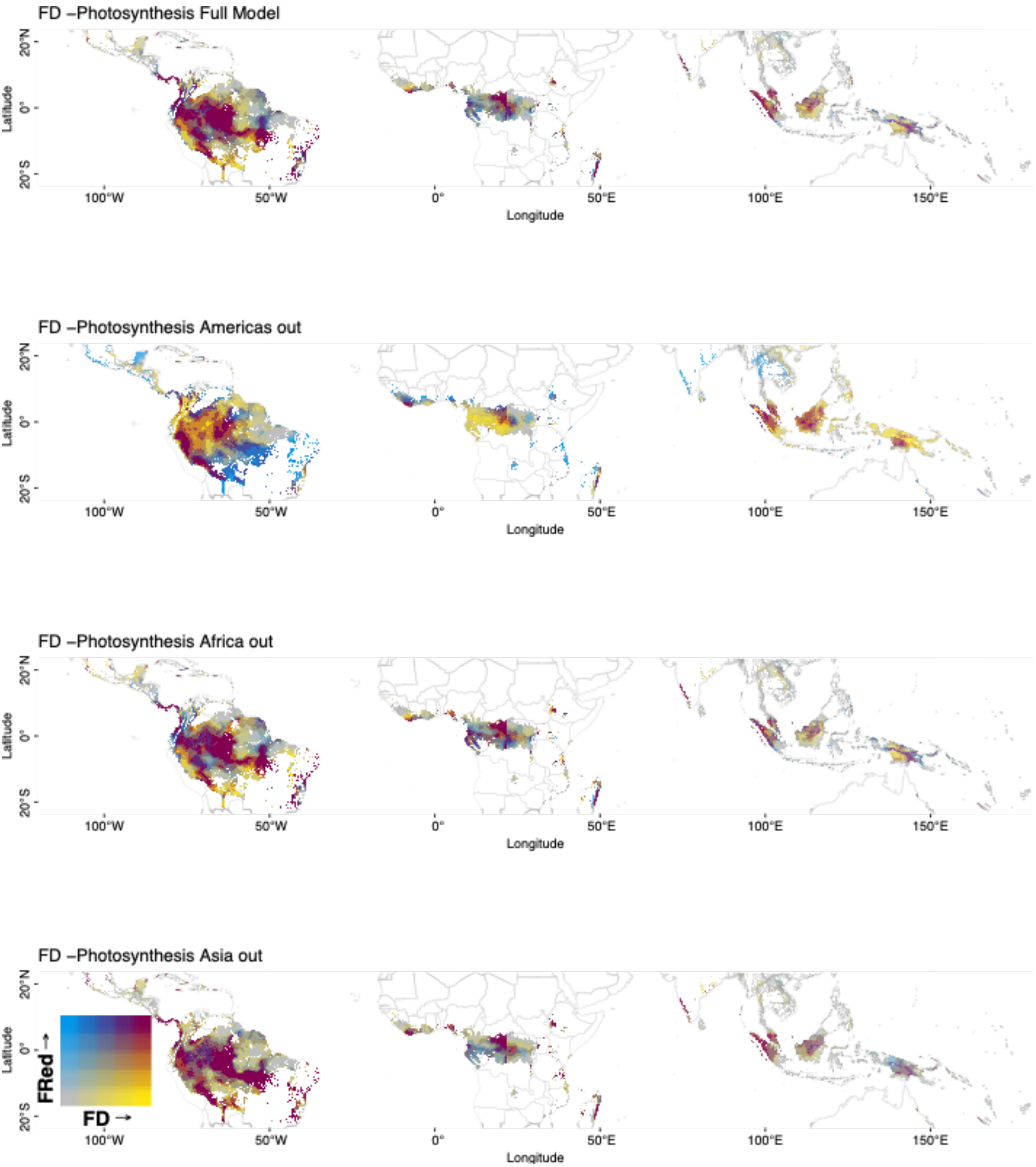

Figure S9. Bivariate maps combining the functional diversity (FD) and redundancy (FRed) for the photosynthesis traits. Each map shows the predictions obtained using the full dataset (Full model) and the changes that occur by leaving the plots from each continent out of the model. The second panel shows the spatial predictions when leaving the records from the Americas out of model fitting, the third panel when leaving records from Africa out and the bottom panel when leaving the records from Asia and Australia out from model fitting.

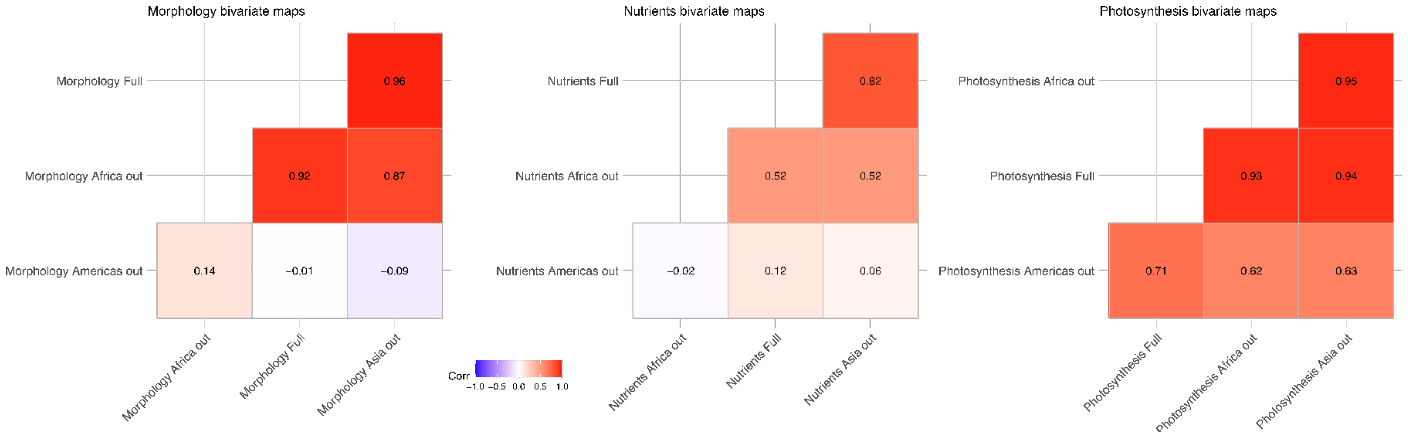

Figure S10. Correlation coefficients between the full model FD-FRed bivariate spatial predictions and those made when plots from one continent out. Overall, when the Americas is left out of model fitting the predictions are most different with the full model predictions and this is due to the higher number of records (plots) coming from this area (see also TS4). When data from the Americas is left out from the morphological and nutrients models the correlation with the full models drops dramatically, suggesting plots in the Americas have unique morphological and nutrients composition (FD-FRed) not found in other areas but also reflects the fact that a large part of the plot data is coming from this area.

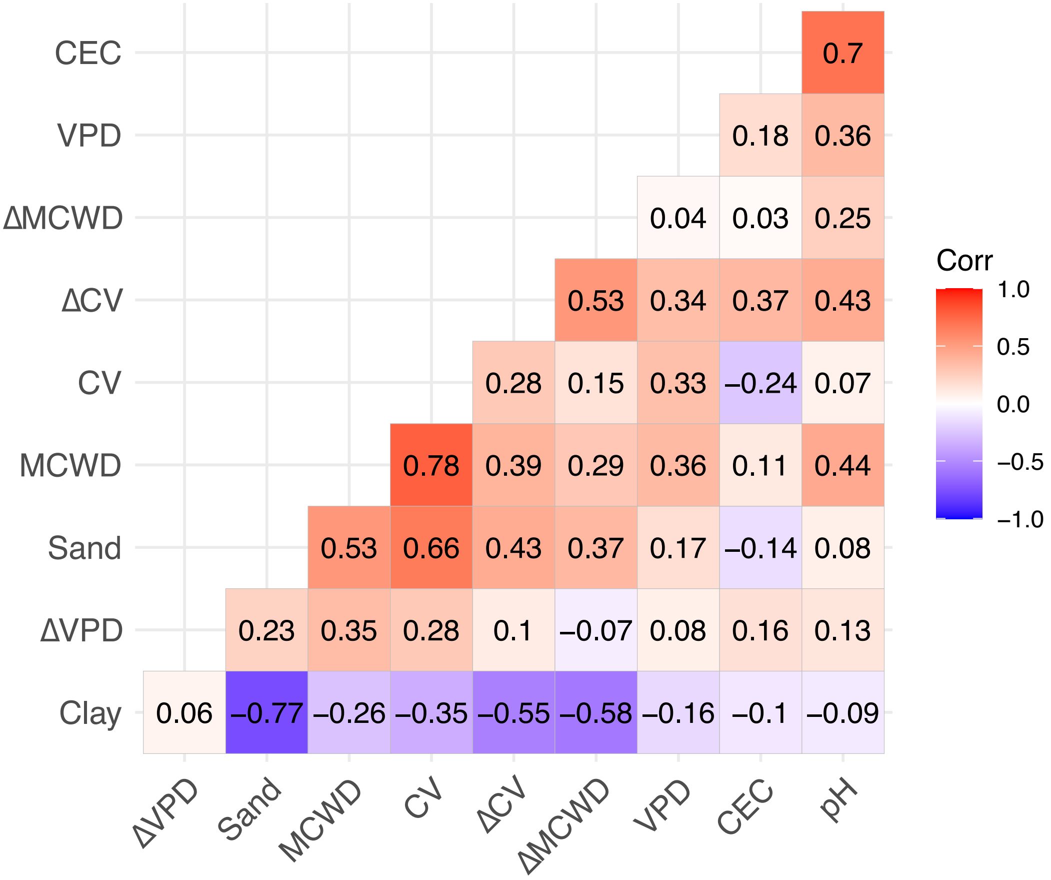

	ΔVPD	Sand	MCWD	CV	ΔCV	ΔMCWD	VPD	CEC	pH
CEC									0.7
VPD								0.18	0.36
ΔMCWD							0.04	0.03	0.25
ΔCV						0.53	0.34	0.37	0.43
CV					0.28	0.15	0.33	−0.24	0.07
MCWD				0.78	0.39	0.29	0.36	0.11	0.44
Sand			0.53	0.66	0.43	0.37	0.17	−0.14	0.08
ΔVPD		0.23	0.35	0.28	0.1	−0.07	0.08	0.16	0.13
Clay	0.06	−0.77	−0.26	−0.35	−0.55	−0.58	−0.16	−0.1	−0.09

Figure S11. Pearson's correlation coefficients between all climatic and soil variables analysed in this study. Besides the correlation between the coefficient of variation of precipitation (CV) and the maximum climatic water deficit (MCWD), cation exchange capacity (CEC) and pH and soil clay content (Clay) and soil sand content (Sand), all other pairwise comparisons had coefficients below 0.70 (our threshold selected to include or exclude a covariate in the model). VPD: vapour pressure deficit. Δ: change.

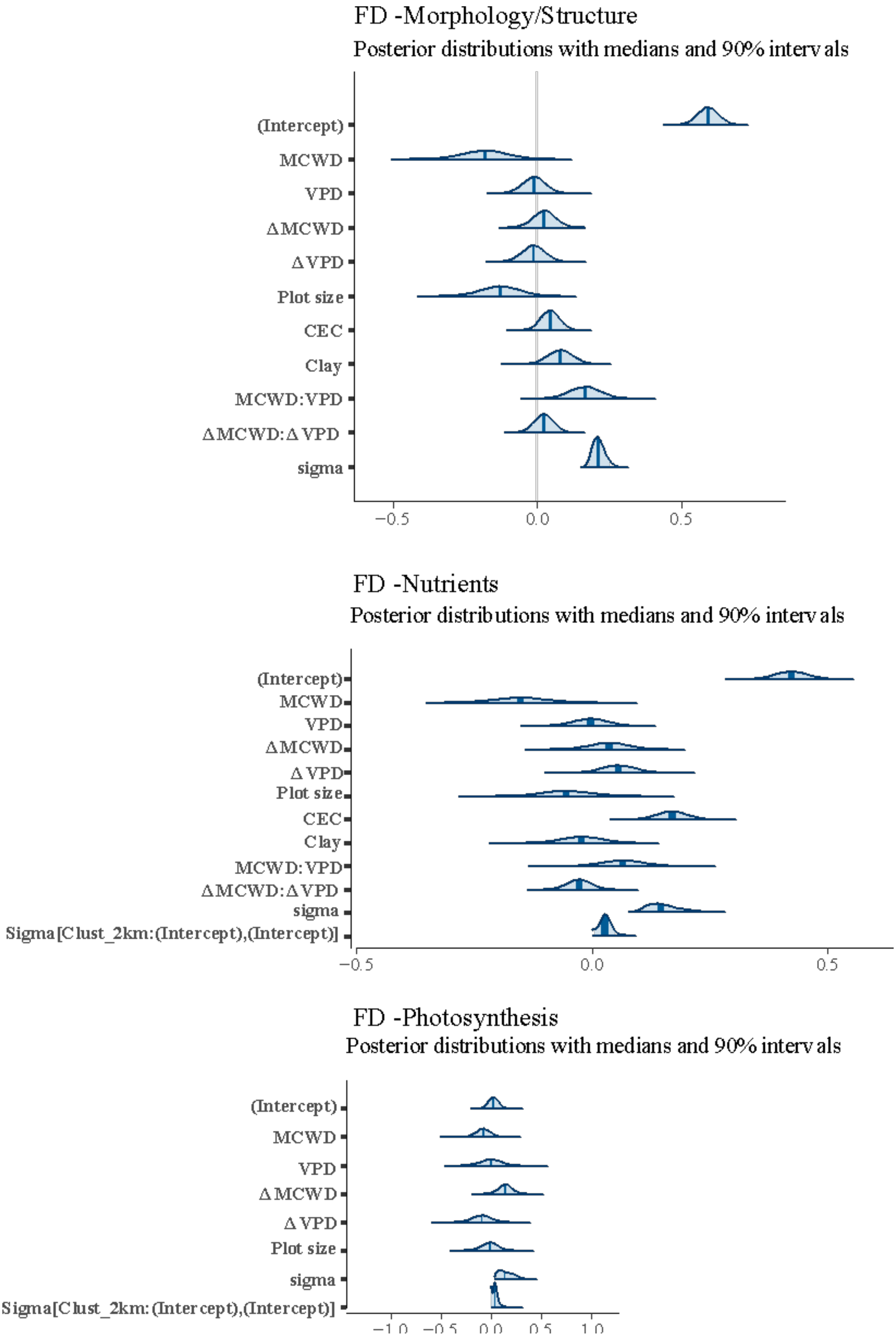

Figure S12. The posterior density distribution of the models fitted exploring the effects of long-term and a changing climate and soil characteristics on the functional diversity (FD) of morphology/structure, nutrients(middle panel) and photosynthesis (bottom panel) traits. The posterior density distribution of the random effect (when included in the model) is not shown for clarity purposes. See Table S3 for full statistical details. MCWD: maximum climatic water deficit, VPD: vapour pressure deficit, CEC: soil cation exchange capacity, Clay: soil clay content. Δ: change.

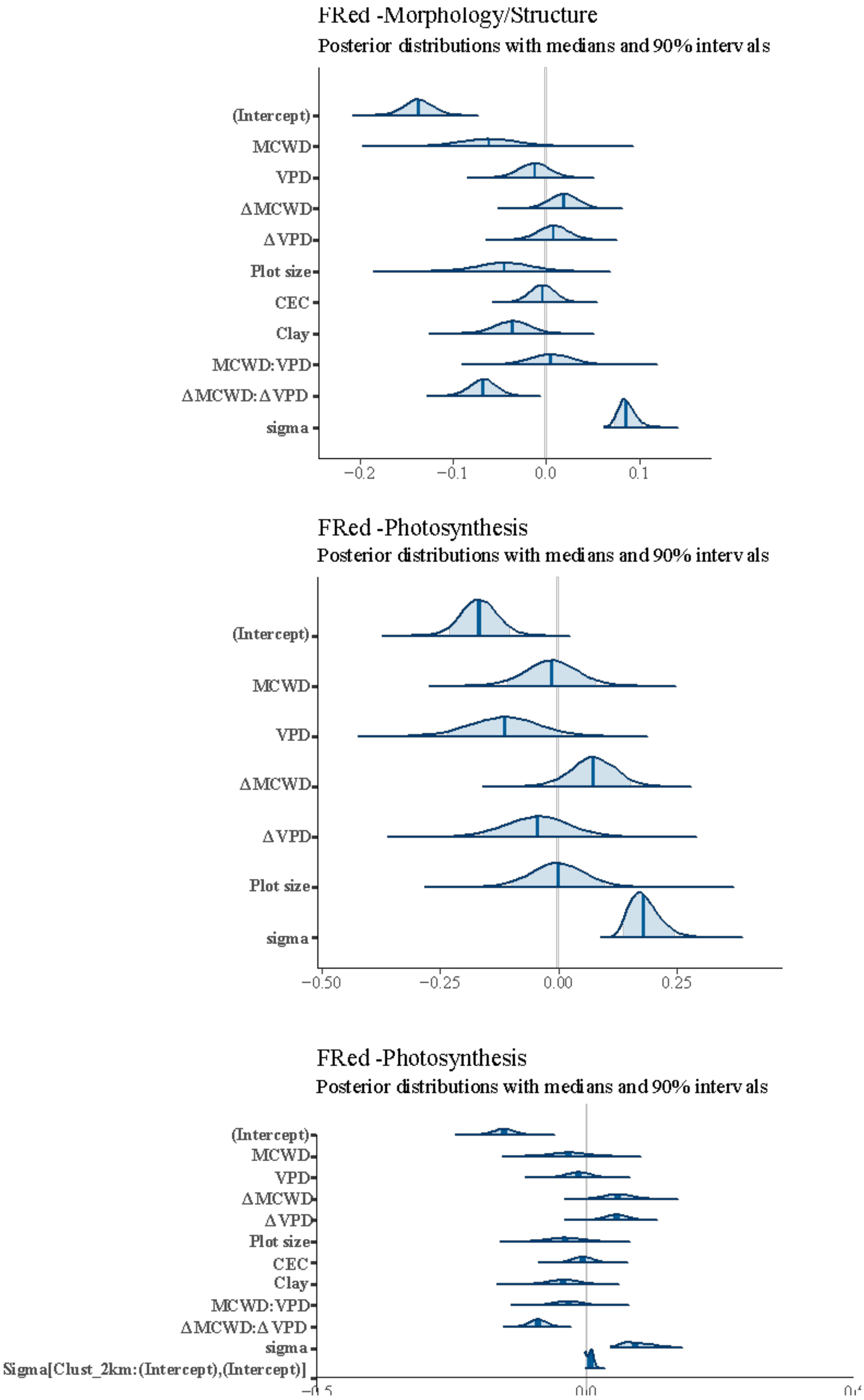

Figure S13. The posterior density distribution of the models fitted exploring the effects of long-term and a changing climate and soil characteristics on the functional redundancy (FRed) of morphology/structure, nutrients(middle panel) and photosynthesis (bottom panel) traits. The posterior density distribution of the random effect (when included in the model) is not shown for clarity purposes. See Table S3 for full statistical details. MCWD: maximum climatic water deficit, VPD: vapour pressure deficit, CEC: soil cation exchange capacity, Clay: soil clay content. Δ: change.

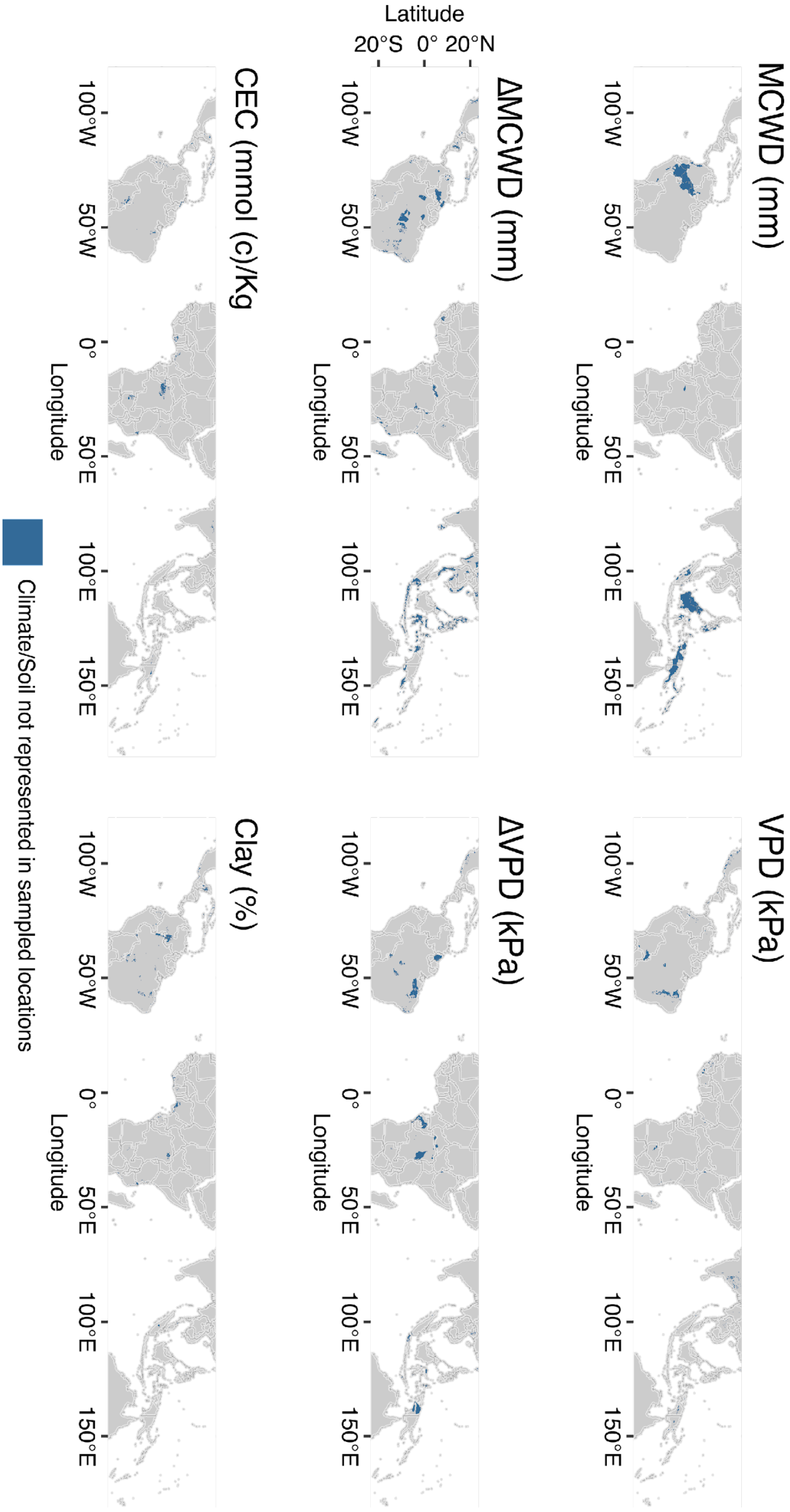

Figure S14. The blue colour shows the distribution of locations that contain climatic and soil values out of the range used to fit the statistical models of functional diversity (FD) and functional redundancy (FRed). The results of FD and FRed scores for those areas (in blue) should be interpreted with caution. See Figure 3 and Figure 4 for the FD and FRed spatial predictions. MCWD: maximum climatic water deficit, VPD: vapour pressure deficit, CEC: soil cation exchange capacity, Clay: soil clay content. Δ: change.

Supplementary Information: Supplementary Tables S1 to S9

Functional susceptibility of tropical forests to climate change

Jesús Aguirre-Gutiérrez et al.

Supplementary Table S1. Plant functional traits included in the analysis, their description and their hypothesised response and importance under a drying climate. References are not exhaustive (see end of document for full details of references).

Functional group	Trait	Description	Importance and hypothesised response to a drying climate	References
Morphology and structure	Leaf area: A (cm^2)	Area of the leaf determined by scanning the adaxial side of the leaf lamina on a flatbed scanner Canon LiDE220®	Relevant as a main light capture mechanism. Higher leaf area could result in more leaf transpiration and thus water loss under a drying climate. Under a drying climate it may increase in deciduous species and expect decreases in evergreens as to limit water loss by transpiration and for increasing cooling.	1,2
	DM: leaf dry mass (g)	Leaf fresh mass calculated as the fresh weight of the recently obtained leaves.	Increasing droughts may cause decreases in leaf dry and fresh mass. Such decreases in leaf dry and fresh mass may have negative implications for biomass productivity.	3
	FM: leaf fresh mass (g)	Leaf dry mass determined after oven drying at 60 °C leaves for 72 hours or until constant weight.		
	LDMC: leaf dry matter content (mg/g)		It is an indicator if leaf defence against drying conditions. It would tend to increase as water stress increases.	4
	LWC (%)	Water content in the leaf determined by subtracting the dry mass content from the fresh mass, multiplying by 100 and dividing by the fresh mass to obtain percentage water content.	Indicator of leaf water stress which can limit photosynthesis and thus productivity. LWC is expected to decline with increasing drought conditions as to avoid leaf water loss.	5
	SLA (m^2/g)	Specific leaf area calculated as the one-sided area of a leaf divided by dry mass	Important for photosynthetic capacity, light capture, water loss, net assimilation rate, leaf life span. May increase if acquisitive species, e.g. deciduous species, become more abundant with a drying climate.	6,7,8

	T (mm)	Thickness of leaf lamina measured by taking four micrometre measurements halfway between the mid-vein and the edge of the leaf, avoiding major secondary veins.	Trade-off between decreasing water transpiration at the expense of higher construction investment. May decrease under a drying climate as a result of increasing in deciduous species which may tend to have thinner leaves. It is expected that thicker leaves become more common under larger water deficits for evergreen species but may decreases for acquisitive deciduous species.	1,2
	WD (g/cm^3).	Wood density obtained from the oven dried wood mass divided by its fresh volume	Relevant for mechanical strengths, stem vulnerability to xylem cavitation. Expected to be higher in areas with lower water resources, and thus increase with a drying climate.	8,9,10,11
	Ca: leaf calcium (%)	Leaf nutrients concentration in percentage obtained from dry leaf samples. On a different branch, all leaves were removed for bulk chemical analysis at different laboratories depending on the traits campaign.	Calcium is a regulator in processes related to growth such as stomatal function, cell division, cell wall synthesis, repair of damage from biotic and abiotic stress. Deacreases in Ca are expected under increasing droughts	12
	K: leaf potassium (%)		Important role in the regulation of water status, make a major contribution to the osmotic potential of cells and tissues and it is involved in physiological processes, such as photosynthesis, osmoregulation and stomatal movement. Based on recent literature It is expected a decreae in leaf K content with increasing drought.	13,14
	Mg: leaf magnesium (%)		Important element for plant growth and photosynthesis which can be impacted by increasing droughts. It has major role in synthesis of proteins, ATP and chlorophyll. It is	15,16

			expected that decreases in Mg may lead to decreases in plant biomass if Mg levels are disrupted by a changing climate.	
	N: leaf nitrogen (%)		Essential for metabolic reactions involved in light capture, photosynthetic capacity and growth. Restricted availabilities limit plant carbon acquisition and growth. Drought effects may be compensated if nitrogen fixing species (mainly Fabaceae) become more abundant. Following the literature it is expected that leaf nitrogen content will decrease with increasing temperature and droughts.	17,18,19,20
	P: leaf phosphorus (%)		Needed nutrient for metabolic reactions that include light capture, related to photosynthetic capacity and growth. Lack of P may limit carbon acquisition and growth. Decreases under a drying climate and possible not strong effect under short term droughts or in wet forests. May be more dependent on soil conditions than on climate.	18,19,20
Photosynthesis	Amax (μmol m^{-2} s^{-1})	Amax: Light-saturated maximum rates of net photosynthesis at saturated CO2. Asat: Light-saturated rates of net photosynthesis at ambient CO2 concentration. Photosynthetic capacity (light-saturated net assimilation rate) was measured at both saturating CO2 concentration (2000 ppm CO2; Amax), and at ambient CO2 concentration (400	Maximum CO2 assimilation. Index of leaf photosynthetic capacity. Higher for species with fast resources turnover, e.g. deciduous vs evergreens. Increase with abundance of such species.	21,22
	Asat (μmol m^{-2} s^{-1})		Saturated photosynthetic rate. Index of leaf photosynthetic capacity. Declines with higher temperatures and lower precipitation. However, Asat is also dependent on CO2 fertilization and N and P levels.	21,22

	RDark (µmol m^{-2} s^{-1})	ppm CO2; Asat) under saturating light conditions and at a temperature of 25 ◦C using a LICOR 6400-XT. RDark: Leaf dark respiration.	Component of plant carbon balance which can return 40–50% of photosynthetically fixed carbon to the atmosphere. Increases in RDark with increases in temperature and decreases in precipitation.	23,24

Supplementary Table S2. Climatic conditions for the full term period (1958-2017) , for its changes between the first (1958-1987) and second (1988-2017) time period analysed and for soil conditions. The third to fifth columns in the table describe if the plot was included (Y) or not (empty) in the FD and FRed analysis for the different functional groups.

Location	Plot	Functional indices Morphology/Structure	Functional indices Nutrients	Functional indices Photosynthesis	Plot size (ha)	MCWD (mm)	VPD (kPa)	CV (mm)	ΔVPD (kPa)	ΔCV (mm)	ΔMCWD (mm)	CEC (mmol (c)/kg)	Clay (%)	pH	Sand (%)
Australia	EP43		Y	Y	0.5	542.25	0.74	0.73	-0.01	-0.07	-40.06	13.78	42.15	5.00	32.33
Australia	AEP02		Y		0.5	671.04	0.75	0.81	-0.01	-0.06	-46.90	11.99	35.74	4.90	35.23
Australia	AEP03		Y	Y	0.5	671.04	0.75	0.91	-0.01	-0.04	-46.90	11.99	35.74	4.80	42.50
Australia	KRU01	Y	Y	Y	0.1	206.56	0.75	0.67	-0.01	-0.09	-58.22	15.34	42.74	5.10	30.70
Australia	AEP41		Y	Y	0.5	386.28	0.71	0.72	0.00	-0.08	-65.35	14.00	36.41	5.00	39.73
Australia	DRO01		Y	Y	0.9	386.28	0.71	0.69	0.00	-0.08	-65.35	14.00	36.41	5.57	38.60
Australia	ROB06		Y	Y	1	460.43	0.72	0.77	-0.01	-0.06	-85.05	13.70	37.11	5.00	33.27
Brazil -NX	VCR02	Y	Y	Y	1	541.76	1.13	0.83	-0.06	0.01	56.21	9.71	25.19	5.40	58.53
Brazil -NX	NXV01	Y	Y	Y	1	524.20	1.11	0.82	-0.06	0.01	40.41	7.77	23.80	5.40	62.50
Brazil -NX	NXV02	Y	Y		1	524.20	1.11	0.82	-0.06	0.01	40.41	7.77	23.80	5.30	63.80
Brazil -NX	NXV10	Y	Y		1	524.20	1.11	0.82	-0.06	0.01	40.41	7.77	23.80	5.37	63.73
Brazil -ST	363_6	Y	Y	Y	0.25	358.87	0.63	0.61	0.02	0.00	-89.87	9.30	36.69	4.03	51.13
Brazil -ST	363_3	Y	Y	Y	0.25	363.17	0.63	0.62	0.02	0.01	-93.20	9.65	34.03	4.07	53.97
Brazil -ST	363_7	Y	Y	Y	0.25	363.17	0.63	0.61	0.02	0.00	-93.20	9.65	34.03	4.13	46.43
Brazil -ST	261_10	Y	Y	Y	0.25	371.36	0.62	0.64	0.02	0.01	-103.91	12.27	50.40	4.07	33.50
Brazil -ST	261_9	Y	Y		0.25	371.36	0.62	0.64	0.02	0.01	-103.91	12.27	50.40	4.30	32.13
Colombia	Macuira	Y	Y		1	941.62	1.22	0.73	0.02	0.04	0.00	20.05	35.18	6.70	34.33
Colombia	Taminango				1	155.61	0.76	0.44	-0.02	0.00	-43.22	25.81	35.12	5.90	31.63
Colombia	Tuparro	Y	Y		1	204.58	1.13	0.70	-0.02	0.01	-75.96	12.61	25.50	5.23	50.37
Colombia	CardonalLoma	Y	Y	Y	1	60.97	1.00	0.41	-0.02	-0.06	-131.07	21.56	41.54	5.00	27.47
Colombia	CardonalPlana		Y		1	60.84	1.08	0.40	-0.03	-0.07	-135.37	19.48	41.67	5.00	24.97
Colombia	Jabiru	Y	Y	Y	1	60.84	1.08	0.44	-0.03	-0.06	-135.37	19.48	41.67	5.20	24.87
Colombia	Tambor	Y	Y		1	57.41	1.05	0.37	-0.03	-0.07	-140.04	18.15	39.63	5.17	26.70
Colombia	Vinculo	Y	Y		1	80.81	0.65	0.37	-0.03	-0.04	-144.66	23.85	34.67	6.03	27.77
Colombia	Cotove		Y		1	152.12	0.83	0.46	-0.06	-0.05	-152.89	19.65	39.04	5.90	34.13
Gabon	MNG04	Y	Y	Y	1	241.18	0.52	0.68	0.06	0.00	32.87	15.35	28.76	4.87	46.00
Gabon	LPG02		Y	Y	1	173.72	0.74	0.68	0.08	-0.01	0.33	13.15	31.79	5.10	56.17
Gabon	LPG01	Y	Y	Y	1	173.93	0.79	0.67	0.08	-0.01	-0.35	12.14	27.79	4.90	54.10
Ghana	KOG03	Y	Y		1	493.04	1.03	0.60	0.02	0.02	-27.55	34.00	21.10	5.53	49.77
Ghana	KOG04	Y	Y		1	493.04	1.03	0.60	0.02	0.02	-27.55	34.00	21.10	5.63	48.57
Ghana	KOG05		Y		1	493.04	1.03	0.60	0.02	0.02	-27.55	34.00	21.10	5.67	49.20
Ghana	KOG06	Y	Y		1	493.04	1.03	0.60	0.02	0.02	-27.55	34.00	21.10	5.70	50.23
Ghana	KOG02		Y		1	474.96	1.00	0.59	0.02	0.01	-29.66	34.00	21.36	5.73	56.23
Ghana	BOB01	Y	Y		1	322.92	0.84	0.52	0.02	0.01	-35.93	32.23	21.89	5.67	46.73
Ghana	BOB02	Y	Y		1	322.92	0.84	0.52	0.02	0.01	-35.93	32.23	21.89	5.73	48.90
Ghana	ANK01	Y	Y		1	149.27	0.67	0.68	0.02	-0.03	-190.69	15.76	22.87	4.77	65.33
Ghana	ANK03	Y	Y		1	149.27	0.67	0.66	0.02	-0.03	-190.69	15.76	22.87	4.80	65.10
Malaysia	MLA-01	Y	Y	Y	1	0.00	0.82	0.15	0.03	-0.01	-46.76	18.05	39.01	5.00	32.87
Malaysia	MLA-02	Y	Y	Y	1	0.00	0.77	0.16	0.03	-0.01	-54.91	20.09	41.13	5.00	32.13
Malaysia	DAN-04	Y	Y	Y	1	0.00	0.79	0.16	0.02	-0.01	-87.00	16.81	38.21	5.10	29.67
Malaysia	DAN-05	Y	Y	Y	1	0.00	0.79	0.16	0.02	-0.01	-87.00	16.81	38.21	5.07	31.10
Mexico	ME_14_00358	Y			0.25	873.77	1.05	1.12	0.07	0.07	156.99	22.89	20.57	6.10	60.37
Mexico	ME_14_00359	Y	Y		0.25	873.77	1.05	1.12	0.07	0.07	156.99	22.89	20.57	5.80	60.90
Mexico	ME_14_00360	Y	Y		0.25	873.77	1.05	1.12	0.07	0.07	156.99	22.89	20.57	6.10	64.53
Mexico	ME_14_00361	Y	Y		0.25	873.77	1.05	1.12	0.07	0.07	156.99	22.89	20.57	6.00	60.90
Mexico	ME_14_00362	Y			0.25	873.77	1.05	1.13	0.07	0.06	156.99	22.89	20.57	6.00	65.57
Mexico	ME_23_00144	Y	Y		0.25	481.96	0.86	0.57	0.03	0.01	-36.86	22.10	49.24	7.00	32.90
Mexico	ME_23_00143	Y	Y		0.25	475.67	0.85	0.57	0.03	0.00	-43.16	24.24	50.72	7.10	30.87
Mexico	ME_23_00146	Y	Y		0.25	475.67	0.85	0.58	0.03	0.01	-43.16	24.24	50.72	7.07	33.33
Mexico	ME_23_00147	Y			0.25	482.78	0.84	0.57	0.03	0.00	-43.73	23.97	50.70	7.17	33.47
Mexico	ME_23_00148	Y	Y		0.25	482.78	0.84	0.57	0.03	0.00	-43.73	23.97	50.70	7.17	34.13
Mexico	ME_23_00149	Y	Y		0.25	482.78	0.84	0.57	0.03	0.00	-43.73	23.97	50.70	7.27	34.40
Mexico	ME_23_00145	Y			0.25	468.84	0.84	0.57	0.03	0.00	-49.46	24.26	51.00	7.00	32.60
Mexico	ME_23_00151	Y	Y		0.25	470.85	0.82	0.58	0.03	-0.01	-56.44	24.81	49.25	6.93	32.07
Panama	Fortuna-AF	Y	Y		1	210.77	0.28	0.59	-0.02	-0.02	48.42	17.38	35.01	5.10	32.93
Panama	Fortuna-HOR	Y	Y		1	210.77	0.28	0.47	-0.02	-0.03	48.42	17.38	35.01	5.03	32.50
Panama	Fortuna-BON	Y	Y		1	146.78	0.25	0.35	-0.02	-0.02	40.31	17.81	31.30	5.33	38.17
Panama	Fortuna-PAS	Y	Y		1	146.78	0.25	0.39	-0.02	0.00	40.31	17.81	31.30	5.43	40.00
Panama	Fortuna-VERA		Y		1	146.78	0.25	0.39	-0.02	0.00	40.31	17.81	31.30	5.13	32.90
Panama	Fortuna-VERB	Y	Y		1	146.78	0.25	0.40	-0.02	0.00	40.31	17.81	31.30	5.20	33.20
Panama	Fortuna-CHOB		Y		1	202.26	0.28	0.35	-0.02	-0.02	39.09	16.71	33.78	5.10	34.20
Panama	Fortuna-HONA		Y		1	202.26	0.28	0.35	-0.02	-0.02	39.09	16.71	33.78	5.20	34.10
Panama	Fortuna-HONB		Y		1	202.26	0.28	0.35	-0.02	-0.02	39.09	16.71	33.78	5.10	34.47
Panama	Fortuna-PIN	Y	Y		1	202.26	0.28	0.53	-0.02	-0.03	39.09	16.71	33.78	5.00	34.23
Panama	Fortuna-SAM	Y	Y		1	202.26	0.28	0.35	-0.02	-0.02	39.09	16.71	33.78	5.20	33.33
Peru	TAM05	Y	Y		1	152.58	0.84	0.55	-0.02	0.02	104.09	12.13	25.13	4.97	36.67
Peru	TAM06	Y	Y		1	152.58	0.84	0.54	-0.02	0.02	104.09	12.13	25.13	5.07	35.33
Peru	SPD01	Y	Y		1	254.08	0.68	0.45	-0.03	0.07	17.55	26.30	28.39	5.20	32.90
Peru	TRU04	Y	Y		1	254.08	0.68	0.56	-0.03	0.07	17.55	26.30	28.39	5.80	43.80
Peru	SPD02	Y	Y		1	101.53	0.72	0.45	-0.03	0.06	15.69	23.14	33.69	5.13	33.23
Peru	PAN03	Y	Y		1	0.00	0.87	0.41	-0.03	0.06	0.30	18.99	35.94	5.00	28.80
Peru	PAN02	Y	Y	Y	1	0.00	0.87	0.41	-0.03	0.06	0.06	20.46	35.80	5.23	27.23
Peru	ESP01	Y	Y		1	371.90	0.62	0.63	-0.02	0.07	-16.96	26.47	27.07	6.17	36.40
Peru	WAY01	Y	Y		1	371.90	0.62	0.63	-0.02	0.07	-16.96	26.47	27.07	6.30	40.03
Peru	ACJ01	Y	Y		1	494.13	0.59	0.75	-0.02	0.06	-36.10	22.98	28.56	6.20	42.00

Brazil -NX: Nova Xavantina; Brazil -ST: Santarem; Malaysia: Malaysian Borneo. Y= yes, used for the FD/FRed calculations. MCWD: maximum climatic water deficit, VPD: vapour presure deficit, CEC: soil cation exchange capacity, Clay: soil clay content. Δ: change.

Supplementary Table S3. Models results testing for the relation of functional diversity (FD) and functional redundancy (FRed) with long-term (MCWD and VPD) and changes in climate (ΔMCWD and ΔVPD) and soil cation exchange capacity (CEC) and clay content (Clay). Important terms (Highest Density Interval does not overlap 0) are highlighted in grey. N refers to the number of vegetation plots used to fit the models. MCWD: maximum climatic water deficit, VPD: vapour pressure deficit, CEC: soil cation exchange capacity, Clay: soil clay content. Δ: change.

Metric	Trait	Parameter	Median	HDI-L	HDI-H	pd	ROPE (%)	Rhat	ESS	R2	N
FD	Morphology / Structure	Intercept	0.590	0.530	0.660	1.00	0.00	1.00	11776.94	0.44	59
		MCWD	-0.180	-0.310	-0.050	0.99	0.01	1.00	6078.76		
		VPD	-0.010	-0.080	0.050	0.60	0.91	1.00	9024.43		
		ΔMCWD	0.030	-0.040	0.090	0.74	0.81	1.00	13793.30		
		ΔVPD	-0.010	-0.080	0.050	0.62	0.89	1.00	11322.42		
		Plot size	-0.130	-0.240	-0.020	0.97	0.10	1.00	5927.16		
		CEC	0.050	-0.010	0.100	0.92	0.65	1.00	10472.41		
		Clay	0.080	0.010	0.160	0.96	0.27	1.00	8307.24		
		MCWD:VPD	0.170	0.080	0.260	1.00	0.00	1.00	7965.82		
		ΔMCWD:ΔVPD	0.020	-0.030	0.080	0.75	0.86	1.00	11051.42		
	Nutrients	Intercept	0.420	0.370	0.480	1.00	0.00	1.00	6860.33	0.75	70
		MCWD	-0.150	-0.240	-0.060	1.00	0.00	1.00	5386.58		
		VPD	0.000	-0.060	0.060	0.54	0.85	1.00	7137.43		
		ΔMCWD	0.040	-0.030	0.110	0.81	0.58	1.00	6996.22		
		ΔVPD	0.060	0.000	0.120	0.94	0.35	1.00	6691.61		
		Plot size	-0.050	-0.140	0.040	0.85	0.42	1.00	5531.48		
		CEC	0.170	0.120	0.220	1.00	0.00	1.00	8388.50		
		Clay	-0.020	-0.090	0.050	0.69	0.70	1.00	6807.73		
		MCWD:VPD	0.060	-0.010	0.140	0.92	0.31	1.00	6358.19		
		ΔMCWD:ΔVPD	-0.030	-0.070	0.010	0.86	0.76	1.00	8657.60		
	Photosynthesis	Intercept	0.020	-0.070	0.120	0.67	0.40	1.00	3596.67	0.75	22
		MCWD	-0.080	-0.200	0.060	0.84	0.19	1.00	3653.69		
		VPD	0.000	-0.180	0.170	0.51	0.25	1.00	2404.67		
		ΔMCWD	0.140	0.020	0.250	0.98	0.01	1.00	3617.61		
		ΔVPD	-0.090	-0.260	0.070	0.83	0.16	1.00	2635.85		
		Plot size	-0.010	-0.150	0.130	0.55	0.32	1.00	6056.06		
FRed	Morphology / Structure	Intercept	-0.140	-0.160	-0.110	1.00	0.00	1.00	10032.57	0.53	59
		MCWD	-0.060	-0.110	-0.010	0.97	0.01	1.00	5039.35		
		VPD	-0.010	-0.040	0.010	0.78	0.37	1.00	7962.77		
		ΔMCWD	0.020	-0.010	0.050	0.88	0.23	1.00	10881.27		
		ΔVPD	0.010	-0.020	0.040	0.69	0.41	1.00	8045.75		
		Plot size	-0.040	-0.090	0.000	0.94	0.07	1.00	4862.01		
		CEC	0.000	-0.030	0.020	0.60	0.53	1.00	9195.92		
		Clay	-0.040	-0.070	0.000	0.97	0.04	1.00	6962.26		
		MCWD:VPD	0.010	-0.030	0.040	0.59	0.33	1.00	6648.54		
		ΔMCWD:ΔVPD	-0.070	-0.090	-0.040	1.00	0.00	1.00	8911.43		
	Nutrients	Intercept	-0.150	-0.180	-0.120	1.00	0.00	1.00	6764.04	0.73	70
		MCWD	-0.030	-0.090	0.020	0.83	0.18	1.00	4501.18		
		VPD	-0.010	-0.050	0.020	0.72	0.37	1.00	5748.85		
		ΔMCWD	0.060	0.020	0.100	0.99	0.00	1.00	5803.23		
		ΔVPD	0.060	0.020	0.090	1.00	0.00	1.00	6924.62		
		Plot size	-0.040	-0.090	0.020	0.88	0.15	1.00	4675.90		
		CEC	0.000	-0.040	0.030	0.60	0.47	1.00	6382.34		
		Clay	-0.040	-0.080	0.000	0.94	0.08	1.00	5455.13		
		MCWD:VPD	-0.030	-0.080	0.010	0.88	0.18	1.00	5391.84		
		ΔMCWD:ΔVPD	-0.090	-0.110	-0.060	1.00	0.00	1.00	6591.10		
	Photosynthesis	Intercept	-0.170	-0.230	-0.100	1.00	0.00	1.00	11858.06	0.33	22
		MCWD	-0.010	-0.110	0.080	0.60	0.19	1.00	8177.61		
		VPD	-0.110	-0.230	0.01	0.94	0.04	1.00	7547.91		
		ΔMCWD	0.070	-0.010	0.160	0.93	0.05	1.00	9917.27		
		ΔVPD	-0.040	-0.160	0.070	0.74	0.13	1.00	7617.03		
		Plot size	0.000	-0.100	0.100	0.51	0.18	1.00	8701.47		

Supplementary Table S4. Relation between the number of records used to fit the FD and FRed models and the correlation between the resulting binary maps constructed with the full dataset and with records from the Americas, Africa or Asia left out. There is in general a high overall correlation between the number of records used the fit the models and the correlation between the full model and continent out bivariate FD-FRed maps (see Figure 5 and Figures S2-S4).

Index	Trait	Comparisons	Overal correlation	Records used	Correlation with full model
FD	Morphology/Structure	Full model	0.99	59	1.00
		Americas out		14	0.21
		Africa out		49	0.95
		Asia out		55	0.98
	Nutrients	Full model	0.81	70	1.00
		Americas out		23	0.34
		Africa out		58	0.47
		Asia out		59	0.86
	Photosynthesis	Full model	0.51	22	1.00
		Americas out		13	0.65
		Africa out		19	0.94
		Asia out		12	0.97
FRed	Morphology/Structure	Full model	0.99	59	1.00
		Americas out		14	-0.50
		Africa out		49	0.91
		Asia out		55	0.94
	Nutrients	Full model	0.99	70	1.00
		Americas out		23	-0.57
		Africa out		58	0.48
		Asia out		59	0.71
	Photosynthesis	Full model	0.65	22	1.00
		Americas out		13	0.23
		Africa out		19	0.99
		Asia out		12	0.84

Table S5. Relationship between FD and FRed levels and taxonomic diversity at the plot level.

Index	Trait group	Taxonomical comparison	Correlation	Pval
FD	Morphology/Structure	Species	0.02	0.90
		Genus	0.06	0.64
		Family	0.12	0.37
	Nutrients	Species	0.02	0.88
		Genus	0.08	0.51
		Family	-0.04	0.74
	Photosynthesis	Species	0.30	0.18
		Genus	0.41	0.06
		Family	0.50	0.02
FRed	Morphology/Structure	Species	0.57	<0.001
		Genus	0.59	<0.001
		Family	0.56	<0.001
	Nutrients	Species	0.49	<0.001
		Genus	0.49	<0.001
		Family	0.43	<0.001
	Photosynthesis	Species	0.36	0.10
		Genus	0.36	0.10
		Family	0.19	0.39

Correlation: Pearson correlation coefficient; P-val: Significance of the correlation

Supplementary Table S6. Percentage of the study area with low, intermediate and high functional diversity and functional redundancy scores. For details about the methodology to obtain the % values show see the methods section in the main text.

Index	Trait	Low (%)	Intermediate (%)	High (%)
FD	Photosynthesis	36.8	60.7	2.4
	Nutrients	14.8	71.1	14.1
	Morphology/Structure	30.4	64.1	5.5
FRed	Morphology/Structure	5.5	92.2	2.3
	Photosynthesis	16.9	76.3	6.8
	Nutrients	3.7	89.2	7.0

Supplementary Table S7. Linear models results explaining the change in AGB after the 2015 El Niño event in African tropical forest. The original data on pre and post El Niño AGB was obtained from Bennet et al. 2021. We modelled the change in AGB as a function of the morphological/structural, leaf nutrients and photosynthetic functional diversity (FD) and redundancy (FRed) map scores (extracted from Figures 3 and 4 in the main text) and their interaction with changes in MCWD and VPD. Several parameters using from the different trait groups have a clear effect (Highest Density Intervals (HDI) do not overlap 0) on the changes in AGB.

Trait	Parameter	Median	HDI-L	HDI-H	pd	ROPE (%	Rhat	ESS	R2	N
Morphology / Structure	Intercept	9.66	8.2	11.1	1.00	0.00	1.000	8051.41	0.18	86
	FD	1.97	0.28	3.65	0.97	0.05	1.000	4014.49		
	FRed	-1.78	-3.55	0.15	0.94	0.12	1.001	3814.73		
	ΔMCWD	-0.9	-2.52	0.75	0.81	0.36	1.001	3984.14		
	ΔVPD	-1.05	-2.89	0.73	0.83	0.30	1.000	4673.00		
	Plot size	-0.25	-1.51	0.97	0.63	0.61	1.000	7001.04		
	FD:ΔMCWD	-0.43	-2.71	1.95	0.62	0.36	1.000	5010.76		
	FRed:ΔMCWD	-0.07	-3.06	3.1	0.51	0.29	1.001	3776.35		
	FD:ΔVPD	-1.42	-3.24	0.33	0.91	0.20	1.001	3358.34		
	FRed:ΔVPD	-0.46	-3.3	2.5	0.60	0.28	1.001	3876.24		
Nutrients	Intercept	10.89	9.4	12.4	1.00	0.00	1.000	5441.02	0.19	
	FD	-1.79	-3.69	0.06	0.94	0.10	1.000	4233.05		
	FRed	-0.89	-2.12	0.39	0.88	0.34	1.000	7212.75		
	ΔMCWD	-2.33	-4.03	-0.57	0.99	0.00	1.001	4690.78		
	ΔVPD	-1.03	-2.69	0.79	0.83	0.30	1.000	4371.06		
	Plot size	-0.92	-2.21	0.39	0.88	0.33	1.000	6570.48		
	FD:ΔMCWD	2.94	0.25	5.69	0.96	0.03	1.000	5389.38		
	FRed:ΔMCWD	-1.87	-3.39	-0.09	0.96	0.08	1.000	4873.43		
	FD:ΔVPD	-0.94	-2.71	0.74	0.81	0.33	1.000	4521.17		
	FRed:ΔVPD	-0.69	-2.89	1.55	0.69	0.34	1.000	5166.57		
Photosynthesis	Intercept	8.44	6.89	9.96	1.00	0.00	1.000	5675.56	0.19	
	FD	-4.13	-10.27	2.22	0.86	0.08	1.001	2072.73		
	FRed	2.96	0.94	5.13	0.99	0.00	1.001	2850.44		
	ΔMCWD	-0.86	-5.89	4.27	0.61	0.18	1.001	2650.77		
	ΔVPD	0.25	-2.33	2.62	0.57	0.35	1.001	2689.94		
	Plot size	-0.21	-1.43	0.98	0.62	0.64	1.000	7324.20		
	FD:ΔMCWD	0.77	-0.74	2.3	0.81	0.41	1.000	3439.71		
	FRed:ΔMCWD	-0.85	-2.5	0.75	0.81	0.37	1.000	3613.87		
	FD:ΔVPD	-3.13	-6.2	-0.19	0.96	0.03	1.000	3598.22		
	FRed:ΔVPD	0.47	-1.66	2.73	0.65	0.37	1.001	3019.23		

HDI: highest density interval, l: low, h: high, pd: probability of direction, Rhat: potential scale reduction statistic, ESS: effective sample size. MCWD: maximum climatic water deficit, VPD: vapour presure deficit, CEC: soil cation exchange capacity, Clay: soil clay content. Δ: change.

Supplementary Table S8. Leave-one-out comparisons results comparing models for the same Index and trait group with and without soil data. The inclusion of soil data improved model outcome for morphology/Structural and Nutrients models but not for the Photosynthesis models. The best model was selected as the one with the lowest LOOIC.

Index	Trait	Climate	Soil	ELPD diff	ELPD LOO	SE ELPD LOO	P LOO	SE P LOO	LOOIC	SE LOOIC
FD	Morphology/Structure	Yes	Yes	0	11.35	5.56	10.93	2.70	-22.71	11.12
		Yes	No	-0.84	10.51	6.09	9.47	2.86	-21.03	12.18
	Nutrients	Yes	Yes	0	6.00	5.41	38.61	4.17	-11.99	10.83
		Yes	No	-7.49	-1.50	5.91	46.18	4.97	2.99	11.81
	Photosynthesis	Yes	Yes	-2.31	-7.29	6.91	25.49	6.41	14.57	13.82
		Yes	No	0	-4.98	7.56	28.72	7.20	9.95	15.13
FRed	Morphology/Structure	Yes	Yes	0	87.44	6.71	9.57	2.03	-174.87	13.41
		Yes	No	-4.65	82.78	7.08	7.85	1.80	-165.56	14.15
	Nutrients	Yes	Yes	-0.24	71.63	9.79	19.09	4.87	-143.27	19.57
		Yes	No	0	71.87	9.57	18.14	4.76	-143.75	19.14
	Photosynthesis	Yes	Yes	0	25.11	3.67	9.89	2.40	-50.22	7.35
		Yes	No	-0.06	25.05	4.03	7.91	2.22	-50.10	8.05

LOOIC: Leave one out information criterion; ELPD LOO: Leave one out expected log predicted density; ELPD diff: difference in expected log predicted density; P LOO: Effective number of parameters; SE LOOIC: standard error of LOOIC; SE ELPD LOO: Standard Error of ELPD; SE P LOO: Standard error of P.

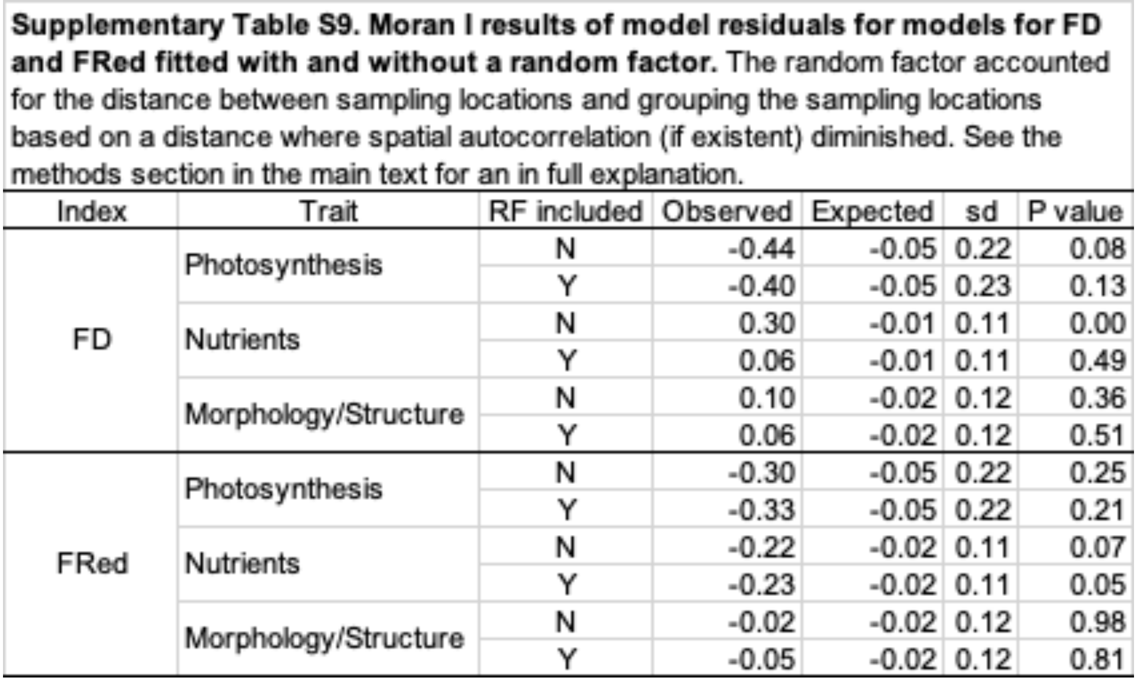

Supplementary Table S9. Moran I results of model residuals for models for FD and FRed fitted with and without a random factor. The random factor accounted for the distance between sampling locations and grouping the sampling locations based on a distance where spatial autocorrelation (if existent) diminished. See the methods section in the main text for an in full explanation.

Index	Trait	RF included	Observed	Expected	sd	P value
FD	Photosynthesis	N	-0.44	-0.05	0.22	0.08
		Y	-0.40	-0.05	0.23	0.13
	Nutrients	N	0.30	-0.01	0.11	0.00
		Y	0.06	-0.01	0.11	0.49
	Morphology/Structure	N	0.10	-0.02	0.12	0.36
		Y	0.06	-0.02	0.12	0.51
FRed	Photosynthesis	N	-0.30	-0.05	0.22	0.25
		Y	-0.33	-0.05	0.22	0.21
	Nutrients	N	-0.22	-0.02	0.11	0.07
		Y	-0.23	-0.02	0.11	0.05
	Morphology/Structure	N	-0.02	-0.02	0.12	0.98
		Y	-0.05	-0.02	0.12	0.81

References for Table S1	Names
1	Lázaro-Nogal A, Matesanz S, Godoy A, Pérez-Trautman F, Gianoli E, Valladares F. Environmental heterogeneity leads to higher plasticity in dry-edge populations of a semi-arid chilean shrub: Insights into climate change responses. J Ecol. (2015);103(2):338-50.
2	Greenwood S, Ruiz-Benito P, Martínez-Vilalta J, Lloret F, Kitzberger T, Allen CD, et al. Tree mortality across biomes is promoted by drought intensity, lower wood density and higher specific leaf area. Ecol Lett. (2017);20(4):539-53.
3	Habermann, E., Dias de Oliveira, E. A., Contin, D. R., Delvecchio, G., Viciedo, D. O., de Moraes, M. A., ... & Martinez, C. A. Warming and water deficit impact leaf photosynthesis and decrease forage quality and digestibility of a C4 tropical grass. Physiologia Plantarum (2019), 165(2), 383-402.
4	Van der Sande, M. T., Arets, E. J., Peña-Claros, M., de Avila, A. L., Roopsind, A., Mazzei, L., ... & Poorter, L. Old-growth Neotropical forests are shifting in species and trait composition. Ecological Monographs (2016), 86(2), 228-243.
5	Jin, X., Shi, C., Yu, C. Y., Yamada, T., & Sacks, E. J.. Determination of leaf water content by visible and near-infrared spectrometry and multivariate calibration in Miscanthus. Frontiers in plant science (2017), 8, 721.
6	Cornelissen JH, Perez-Harguindeguy N, Díaz S, Grime JP, Marzano B, Cabido M, et al. Leaf structure and defence control litter decomposition rate across species and life forms in regional floras on two continents. New Phytol. (1999);143(1):191-200.
7	Poorter L, McDonald I, Alarcón A, Fichtler E, Licona J, Peña-Claros M, et al. The importance of wood traits and hydraulic conductance for the performance and life history strategies of 42 rainforest tree species. New Phytol. (2010);185(2):481-92.
8	Lohbeck M, Poorter L, Paz H, Pla L, van Breugel M, Martínez-Ramos M, et al. Functional diversity changes during tropical forest succession. Perspect Plant Ecol Evol Syst. (2012);14(2):89-96.
9	Poorter L, Hawthorne W, Bongers F, Sheil D. Maximum size distributions in tropical forest communities: Relationships with rainfall and disturbance. J Ecol. (2008);96(3):495-504.
10	Chave J, Coomes D, Jansen S, Lewis SL, Swenson NG, Zanne AE. Towards a worldwide wood economics spectrum. Ecol Lett. (2009);12(4):351-66.

11 Markesteijn L, Poorter L, Paz H, Sack L, Bongers F. Ecological differentiation in xylem cavitation resistance is associated with stem and leaf structural traits. Plant, Cell Environ. (2011);34(1):137-48.

12 Lautner, S., & Fromm, J. Calcium-dependent physiological processes in trees. Plant Biology (2010), 12(2), 268-274.

13 Barker, Allen V., and David J. Pilbeam, eds. Handbook of plant nutrition. CRC press, 2015; Mengel K, Kirkby EA (2001) Principles of Plant Nutrition (4th Edn), International Potash Institute, Switzerland, 687 pp.

14 León-Sánchez, Lupe, et al. "Altered leaf elemental composition with climate change is linked to reductions in photosynthesis, growth and survival in a semi-arid shrubland." Journal of Ecology 108.1 (2020): 47-60.

15 da Silva, Elizamar Ciríaco, R. J. M. C. Nogueira, Marcelle Almeida da Silva, and Manoel Bandeira de Albuquerque. "Drought stress and plant nutrition." Plant stress 5, no. 1 (2011), 32-41.

16 Soares, J. C., Santos, C. S., Carvalho, S. M., Pintado, M. M., & Vasconcelos, M. W. Preserving the nutritional quality of crop plants under a changing climate: importance and strategies. Plant and Soil (2019), 443(1), 1-26.

17 Sardans, J., PeNUuelas, J., Estiarte, M., & Prieto, P. Warming and drought alter C and N concentration, allocation and accumulation in a Mediterranean shrubland. Global Change Biology (2008), 14(10), 2304-2316.

18 Elser JJ, Bracken ME, Cleland EE, Gruner DS, Harpole WS, Hillebrand H, et al. Global analysis of nitrogen and phosphorus limitation of primary producers in freshwater, marine and terrestrial ecosystems. Ecol Lett. (2007); 10(12):1135-42.

19 Reich PB, Oleksyn J, Wright IJ, Niklas KJ, Hedin L, Elser JJ. Evidence of a general 2/3-power law of scaling leaf nitrogen to phosphorus among major plant groups and biomes. Proceedings of the Royal Society of London B: Biological Sciences (2010); 277(1683):877-83.

20 He M, Dijkstra FA. Drought effect on plant nitrogen and phosphorus: A meta-analysis. New Phytol. (2014); 204(4):924-31.

21 Sobrado M. Cost-benefit relationships in deciduous and evergreen leaves of tropical dry forest species. Funct Ecol. (1991), 608-16.

22 Mielke MS, Almeida AFd, Gomes FP. Photosynthetic traits of five neotropical rainforest tree species: Interactions between light response curves and leaf-to-air vapour pressure deficit. Brazilian Archives of Biology and Technology. (2005); 48(5):815-24.

23 Wang, X., Lewis, J. D., Tissue, D. T., Seemann, J. R., & Griffin, K. L. Effects of elevated atmospheric CO2 concentration on leaf dark respiration of Xanthium strumarium in light and in darkness. Proceedings of the National Academy of Sciences (2001), 98(5), 2479-2484.

24 Wright, I. J., Reich, P. B., Atkin, O. K., Lusk, C. H., Tjoelker, M. G., & Westoby, M. Irradiance, temperature and rainfall influence leaf dark respiration in woody plants: evidence from comparisons across 20 sites. New Phytologist (2006), 169(2), 309-319.